

# **The BCL-2 Family Member BOK Promotes KRAS-driven Lung Cancer Progression in a p53-dependent Manner**

Anna-Lena Sophia Meinhardt

Vollständiger Abdruck der von der TUM School of Medicine and Health der Technischen Universität München zur Erlangung einer Doktorin der Medizinischen Wissenschaft (Dr. med. sci.) genehmigten Dissertation.

Vorsitz: apl. Prof. Dr. Klaus-Peter Janssen

Prüfende der Dissertation:

1. apl. Prof. Dr. Philipp J. Jost
2. Priv.-Doz. Dr. Roman Nawroth
3. apl. Prof. Dr. Robert Oostendorp

Die Dissertation wurde am 13.06.2024 bei der Technischen Universität München eingereicht und durch die TUM School of Medicine and Health am 04.12.2024 angenommen.

Die vorliegende Dissertation wurde gefördert durch das Promotionsprogramm „Translationale Medizin“ der Medizinischen Fakultät der Technischen Universität München, sowie durch das Mildred-Scheel-Doktorandenprogramm der Deutschen Krebshilfe.



*Research is the process of going up alleys to see if they are blind.*

Marston Bates

*Meinen Eltern.*

## Abstract

---

With over 2 million new diagnoses annually, lung cancer is one of the most commonly diagnosed cancers worldwide (Thai et al., 2021). It is also the leading cause of cancer deaths, resulting in approximately 1.79 million fatalities annually (Global Cancer Observatory: Cancer Today. International Agency for Research on Cancer, 2024; Siegel et al., 2022). While some countries have seen a recent decline in incidence, likely due to slowly decreasing tobacco consumption, the incidence is still rising in low-or-middle-income countries (Bade & Dela Cruz, 2020). Over the past years there has been substantial progress in our understanding of the molecular characteristics and ways to treat lung cancer, specifically non-small cell lung cancer (NSCLC). In addition to surgery, radiation, and traditional cytotoxic chemotherapy, we can now utilize immunotherapy or targeted agents to treat patients (Thai et al., 2021). Important mutations involved in tumorigenesis include the tumor suppressor *TP53*, the GTPase *KRAS* or the receptor tyrosine kinase *EGFR*; the latter two of which can be targeted therapeutically (Thai et al., 2021). Unfortunately, despite these advances, there is still much to be done to improve outcomes for cancer patients.

The process of programmed cell death (apoptosis) has long been understood to be a crucial component in the development and survival of cancer cells (Hanahan & Weinberg, 2000). Specifically, the BCL-2 family of proteins is key in regulating this process, and the balance of pro- and anti-apoptotic members can decide a cell's continued survival, or induce a death cascade through permeabilization of the mitochondrial outer membrane (MOMP) (Cory, Huang, & Adams, 2003). Consequently, multiple family members have been implicated in cancer development, such as BCL-2 in B-cell lymphomas (Warren, Wong-Brown, & Bowden, 2019). One of the more elusive family members, the BCL-2 related ovarian killer (BOK), has been shown to be involved in many different cellular processes, including MOMP, ER stress, DNA damage, and nucleotide synthesis (Naim & Kaufmann, 2020). A wide-ranging study of human cancer tissue and cell lines by Beroukhim et al. found that the locus containing *BOK* was frequently deleted, suggesting that it may be a tumor suppressor (Beroukhim et al., 2010).

In our research using a murine model of *Kras*-driven carcinogenesis, we found that BOK promotes lung cancer progression in a p53-dependent manner. We were able to show that in early stages of tumor development, *Bok*-deficient mice developed fewer numbers of tumors, and that these showed evidence of decreased proliferation and increased levels of DNA damage, compared to *Bok*-proficient animals. Using murine lung cancer cell lines, we could confirm that loss of *Bok* increased cells' susceptibility to DNA damage and death. Intriguingly, the absence of *Bok* did not appear to cause significant differences in more advanced stages of carcinogenesis, with mice showing similar tumor burden and proliferative rates at a later timepoint. Through additional deletion of *TP53* in our transgenic mice, we could demonstrate that the initial phenotype was fully dependent on the presence of p53.

Overall, we were able to show that that presence of the BOK protein promotes proliferation of tumor cells in *Kras*-driven lung cancer, especially in early tumorigenesis, and is vital in cellular response to DNA damage.

# Table of Contents

---

1. Introduction.....	9
1.1 Lung cancer.....	9
1.1.1 Lung cancer incidence.....	9
1.1.2 Screening.....	9
1.1.3 Diagnosis.....	11
1.1.4 Histology.....	11
1.1.5 Molecular basics.....	12
1.1.6 Treatment.....	14
1.2 BCL-2 family.....	15
1.2.1 BCL-2 family and the apoptotic pathway.....	15
1.2.2 BCL-2 family and cancer.....	16
1.3 BCL-2 related ovarian killer “BOK”.....	18
1.4 Mouse models of lung cancer.....	19
1.5 Aims of this project.....	20
2. Materials and Methods.....	23
2.1 Cell culture.....	23
2.2 Inducible BOK overexpression.....	23
2.3 CRISPR/Cas9-mediated genome editing.....	23
2.4 Immunoblotting.....	24
2.5 Quantitative real-time PCR (qPCR).....	24
2.6 Cell proliferation and viability analysis.....	24
2.7 Comet assay.....	25
2.8 Mouse strains.....	25
2.9 Tumor induction.....	25
2.10 Tissue harvesting.....	26
2.11 H&E staining and tumor burden analysis.....	26
2.12 AB-PAS staining.....	26
2.13 Immunohistochemistry (IHC).....	27
2.14 Absorption-based X-ray micro-CT.....	27
2.15 Seahorse assay.....	27

2.16 TCGA data analysis .....	28
2.17 Statistical analysis .....	28
3. Results.....	29
3.1 BOK levels in human lung cancer samples.....	29
3.2 In vitro overexpression of BOK.....	29
3.3 BOK-deficient cell lines show decreased proliferation.....	31
3.4 BOK may have an influence on cellular metabolism.....	32
3.5 BOK-deficiency leads to increased DNA damage in cell lines .....	33
3.6 Generation of <i>Kras</i> <sup>G12D</sup> -driven lung cancer mouse model.....	36
3.7 Characterization of BOK in <i>Kras</i> <sup>G12D</sup> -driven tumorigenesis .....	36
3.8 BOK-deletion decreases tumor burden after 19 weeks of tumorigenesis .....	38
3.9 CT imaging of lungs confirms histologic findings.....	39
3.10 BOK-proficiency leads to higher tumor grades .....	40
3.11 BOK-deficient lesions show decreased proliferative rates .....	42
3.12 More DNA damage is seen in BOK-deficient animals .....	43
3.13 Similar immune infiltration is seen in all genotypes.....	43
3.14 Loss of phenotypic differences upon prolonged tumorigenesis.....	45
3.15 Influence of co-deletion of the tumor suppressor <i>Tp53</i> .....	47
4. Discussion.....	50
5. Outlook .....	56
6. Abbreviations.....	58
7. Acknowledgements.....	61
8. References.....	62

## Published work

Parts of this thesis have previously been published by me in a peer-reviewed journal. Some of the figures that will follow have been adapted from that manuscript.

**Meinhardt, A. L.**, Munkhbaatar, E., Höckendorf, U., Dietzen, M., Dechant, M., Anton, M., Jacob, A., Steiger, K., Weichert, W., Brcic, L., McGranahan, N., Branca, C., Kaufmann, T., Dengler, M. A., & Jost, P. J. (2022). **The BCL-2 family member BOK promotes KRAS-driven lung cancer progression in a p53-dependent manner.** *Oncogene*, *41*(9), 1376-1382. <https://doi.org/10.1038/s41388-021-02161-1>

# 1. Introduction

---

## 1.1 Lung cancer

### 1.1.1 Lung cancer incidence

Lung cancer continues to be one of the most frequently diagnosed cancers and remains the leading cause of cancer deaths worldwide, with five-year survival at only 22% for all stages combined (Global Cancer Observatory: Cancer Today. International Agency for Research on Cancer, 2024; Siegel et al., 2022). In the year 2020, it caused 1.79 million deaths (18%) globally (Global Cancer Observatory: Cancer Today. International Agency for Research on Cancer, 2024). In the United States, more patients die from lung cancer each day than from prostate, breast, and pancreatic cancers combined (Fig. 1B) (Siegel et al., 2022). Public health measures and awareness have led to a slow decrease in incidence in countries such as the United States (Bade & Dela Cruz, 2020; Thai et al., 2021). Over the past decade, total lung cancer incidence has declined by roughly 3% in men (Siegel et al., 2022). In women, however, it only declined by 1%, which is likely due to the historical delay in tobacco use and cessation by women (Siegel et al., 2022; Thai et al., 2021) (Fig. 1A). But while the incidence has been declining in higher income countries, it has been rising in low-or-middle-income countries due to a more recent history of tobacco use (Bade & Dela Cruz, 2020) and lack of public health initiatives for smoking cessation (Thai et al., 2021). Aside from tobacco use, other less common risk factors for lung cancer include ionizing radiation, environmental toxins and polycyclic aromatic hydrocarbons (Duma, Santana-Davila, & Molina, 2019).

### 1.1.2 Screening

Since greater than 80% of lung cancer cases are caused by smoking (Islami et al., 2018), some countries now recommend lung cancer screening with low-dose computed tomography (LDCT) for patients that have a significant smoking history, although exact guidelines vary. In the United States, for example, all patients ages 50 to 80 who are current or former smokers and who smoked at least 20 packyears cumulatively should be offered annual screening, usually done via low-dose CT (Wolf et al., 2024). Other methods of screening, such as circulating tumor DNA in the

peripheral blood (ctDNA) are also being investigated (Thai et al., 2021). The implementation of screening is especially important, since patients often either have no symptoms or only non-specific manifestations, such as cough, shortness of breath, or weight loss, which often do not prompt immediate work-up (Duma, Santana-Davila, & Molina, 2019).

**A**

<b>Estimated new cases - Males</b>			<b>Estimated new cases - Females</b>		
Prostate	268,490	27%	Breast	287,850	31%
Lung and bronchus	117,910	12%	Lung and bronchus	118,830	13%
Colon and rectum	80,690	8%	Colon and rectum	70,340	8%
Bladder	61,700	6%	Uterine corpus	65,950	7%
Melanoma	57,180	6%	Melanoma	42,600	5%
Kidney	50,290	5%	Non-Hodgkin lymphoma	36,350	4%
Non-Hodgkin lymphoma	44,120	4%	Thyroid	31,940	3%
Oral cavity and pharynx	38,700	4%	Pancreas	29,240	3%
Leukemia	35,810	4%	Kidney	28,710	3%
Pancreas	32,970	3%	Leukemia	24,840	3%
<b>All sites</b>	<b>983,160</b>	<b>100%</b>	<b>All sites</b>	<b>934,870</b>	<b>100%</b>

**B**

<b>Estimated deaths - Males</b>			<b>Estimated deaths - Females</b>		
Lung and bronchus	68,820	21%	Lung and bronchus	61,360	21%
Prostate	34,500	11%	Breast	43,250	15%
Colon and rectum	28,400	9%	Colon and rectum	24,180	8%
Pancreas	25,970	8%	Pancreas	23,860	8%
Liver, intrahepatic bile duct	20,420	6%	Ovary	12,810	4%
Leukemia	14,020	4%	Uterine corpus	12,550	4%
Esophagus	13,250	4%	Liver, intrahepatic bile duct	10,100	4%
Bladder	12,120	4%	Leukemia	9,980	3%
Non-Hodgkin lymphoma	11,700	4%	Non-Hodgkin lymphoma	8,550	3%
Brain and nervous system	10,710	3%	Brain and nervous system	7,570	3%
<b>All sites</b>	<b>322,090</b>	<b>100%</b>	<b>All sites</b>	<b>287,270</b>	<b>100%</b>

**Figure 1. Cancer incidence and deaths in the United States.** Ten leading cancer types for the estimated new cancer cases (A) and deaths (B) in the United States in 2022. Adapted from Siegel et al., 2022.

### 1.1.3 Diagnosis

Once suspicion has been raised due to radiographic findings or clinical symptoms, patients undergo staging to determine the extent of their disease and guide the appropriate therapeutic strategy. This will initially consist of radiographic imaging, which can include computed tomography (CT), magnetic resonance imaging (MRI), and/or fluorodeoxyglucose (FDG) positron emission tomography (PET) (National Comprehensive Cancer Network, 2024; Thai et al., 2021). Most important is the histologic confirmation of diagnosis through tissue sampling, which can occur through varying modalities such as bronchoscopy, percutaneous biopsy of peripheral lesions, biopsy of suspected metastatic lesions, or more invasive procedures if indicated (Planchard et al., 2018). Once a formal diagnosis is made, this is usually followed by molecular testing, often next generation sequencing, given the importance of finding targetable mutations for treatment planning (Ionescu et al., 2022). Unfortunately, at the time of diagnosis, most patients are already in later stages of disease, with 22% of patients demonstrating regional lymph node involvement and 57% having metastatic lesions outside the lung (Bade & Dela Cruz, 2020), which significantly limits treatment options and life expectancy.

### 1.1.4 Histology

Based on the 2021 WHO classification, lung cancer is commonly divided into two main categories: non-small cell lung cancer (NSCLC, accounting for ca. 85% of cases) and small cell lung cancer (SCLC, ca. 15%) (Duma, Santana-Davila, & Molina, 2019).

NSCLC is classified into three main subcategories: adenocarcinoma, squamous cell carcinoma, and large cell carcinoma (Fig. 2A) (Duma, Santana-Davila, & Molina, 2019). Classification is done through microscopic analysis of hematoxylin and eosin (H&E)-stained tissue followed by immunohistochemical analysis. Of the different types, the most common one is adenocarcinoma, which accounts for 40% of lung cancers and usually arises in the lung periphery (Duma, Santana-Davila, & Molina, 2019). It is diagnosed by visualizing a neoplastic glandular structure, expression of the pneumocyte marker TTF-1 (thyroid transcription factor-1), or intracytoplasmic mucin (Thunnissen, 2012). Squamous cell carcinomas (SCC), which make up 25-30% of lung cancers, are located more centrally (Duma, Santana-Davila, & Molina, 2019). They are characterized by keratin production of neoplastic cells and/or intercellular desmosomes, or by other typical SCC

markers on IHC such as p40, p63, CK5/6 (Inamura, 2018). Large cell carcinomas, on the other hand, are a diagnosis of exclusion that is made on surgical specimens without squamous, glandular or neuroendocrine differentiation (Pelosi et al., 2015). They represent around 5-10% of lung cancers, and are also found more peripherally. Given the improvement of diagnostic techniques in use, their incidence has been declining over recent years (Duma, Santana-Davila, & Molina, 2019).

Small cell lung cancer, on the other hand, histologically consists of small round or oval cells with minimal cytoplasm that exhibit both lung-specific (e.g. TTF-1), as well as characteristic neuroendocrine markers (such as synaptophysin and CD56). SCLC is predominantly centrally localized and is the most frequent cause of paraneoplastic syndromes in patients (van Meerbeeck, Fennell, & De Ruyscher, 2011).

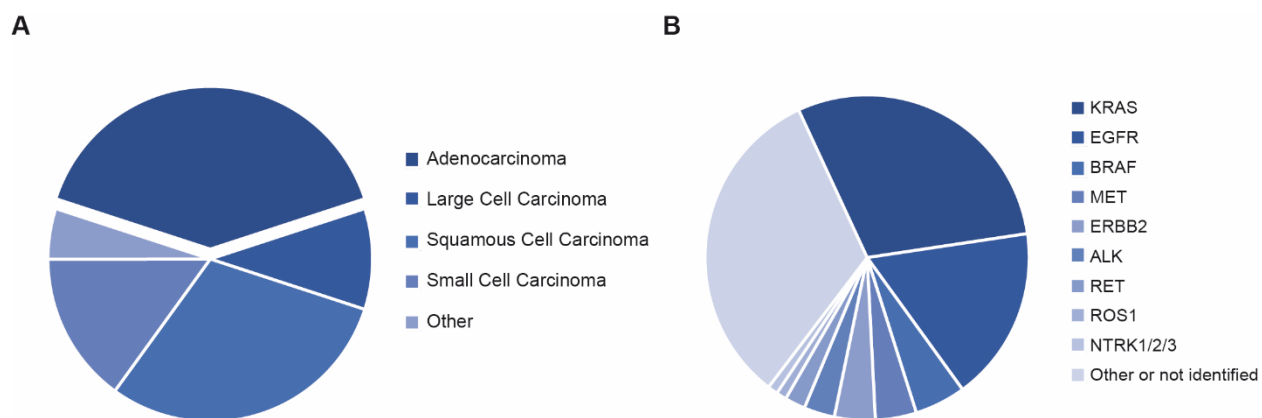


**Figure 2. Lung cancer histology and driver mutations.** (A) Lung cancer is made up of adenocarcinoma (40%), large cell carcinoma (5-10%), squamous cell carcinoma (25-30%), small cell carcinoma (15%) and other (5%). (B) The frequencies of common oncogenic driver mutations in NSCLC are shown based on a cohort of 4064 patients with metastatic NSCLC. Adapted from Singal et al., 2019 and Thai et al., 2021.

### 1.1.5 Molecular basics

The most common mutation in NSCLC, after tumor protein 53 (*TP53*), is Kirsten rat sarcoma *KRAS*, followed by alterations in epidermal growth factor receptor (*EGFR*) and v-raf murine sarcoma viral oncogene homolog B (*BRAF*), as well as *MET* and anaplastic lymphoma kinase (*ALK*) (Fig. 2B) (Chevallier et al., 2021; Thai et al., 2021). Given the improvement of targeted therapies over the recent years, many guidelines now recommend molecular testing as part of the tumor evaluation, especially in patients with advanced disease.

The most frequent mutation in NSCLC is the tumor suppressor *TP53*, which is mutated in approximately half of all patients (Singal et al., 2019; TCGA Research Network, 2014). It has long been known to play a key role in tumorigenesis, as the p53 protein is a nuclear transcription factor that inhibits cell division and survival as part of a cell's response to stressors (Donehower et al., 2019; Hu et al., 2021). The protein transcriptionally targets hundreds of genes and, depending on the cell-specific context, upregulates genes coding for DNA repair proteins, cell cycle inhibitors, apoptosis-inducers, and downregulates genes involved in cell cycle progression. The gene itself is regulated both through binding proteins, as well as through post-translational modification (Donehower et al., 2019). Many tumors with mutations in *TP53* are known to progress more rapidly and often have a poorer prognosis (Donehower et al., 2019; Hu et al., 2021). Efforts to develop pharmacologic strategies of targeting mutated *TP53* and restoring its functions in patients have not yet yielded promising results (Hu et al., 2021).

The *KRAS* gene encodes a membrane-bound small guanosine triphosphate (GTP)ase and affects downstream pathways such as phosphatidylinositol-3-kinase (PI3K) and mitogen-activated protein kinase (MAPK) (Reck et al., 2021). *KRAS* mutations are the most frequently detected oncogenic drivers in NSCLC (found in roughly 30%), have been associated with smoking, and are more prevalent in adenocarcinoma than in squamous NSCLC (Chevallier et al., 2021; Reck et al., 2021). Prognostic implications, however, are unclear. Mutations usually occur in the form of point mutations (notably G12C, G12V and G12D) and there have long been efforts to find targeted *KRAS* agents for treating patients, the first of which was approved for clinical use in 2021 (Chevallier et al., 2021; Reck et al., 2021).

The *EGFR* gene encodes for a receptor tyrosine kinase that, upon binding of ligands, activates the *PI3K/AKT/mTOR* and *RAS/RAF/MEK* pathways (O'Leary et al., 2020). Mutations are found in 17% of NSCLC patients and commonly involve exon 19 deletions or point mutations of codon 858 in exon 21 (Thai et al., 2021). For years now, pharmacologic targeting of *EGFR* mutations has been a successful treatment strategy for cancers of the lung and colon, among others, leading to superior patient outcomes (O'Leary et al., 2020).

Programmed cell death protein 1 (PD1) and programmed death-ligand 1 (PD-L1) are part of a system of immune checkpoints that are used by cancer cells to inactivate T cells (Pawelczyk et al., 2019). Through modulating T cell activity, inhibiting death of regulatory T cells and activating

apoptosis of antigen-specific T cells, this system can facilitate self-tolerance and prevent an immune attack (Han, Liu, & Li, 2020; Pawelczyk et al., 2019). Immunohistochemical analysis of tissue samples can determine the expression of PD-L1 on the surface of tumor cells, which has been found to be a predictive biomarker (Thai et al., 2021). Altering this pathway with PD-1 inhibitors has proven to be a highly effective treatment strategy in lung cancer and many other entities (Thai et al., 2021).

### 1.1.6 Treatment

The initial approach for early-stage NSCLC is usually based on surgical intervention, with anatomical resection (e.g. lobectomy) being the gold standard (Thai et al., 2021). Tumors with more extensive invasion can undergo en-bloc resection of the involved structure, if feasible (National Comprehensive Cancer Network, 2024). Radiotherapy is mostly used in inoperable patients, but can also be considered in the postoperative or palliative setting (National Comprehensive Cancer Network, 2024; Thai et al., 2021). Additionally, adjuvant or neoadjuvant systemic therapy, such as chemotherapy, immune checkpoint inhibitor (ICI) therapy and/or targeted agents, are used in most patients (Thai et al., 2021). Chemotherapy still heavily relies on traditional cytotoxic agents, with most first line regimens including a platinum agent (carbo- or cisplatin, which bind to DNA strands causing crosslinking) among others (National Comprehensive Cancer Network, 2024). Often this is combined with ICIs targeting PD-1/PD-L1 (such as pembrolizumab or atezolizumab) and these are often continued as maintenance therapy for many months (Thai et al., 2021). In patients with advanced or metastatic disease, targeted agents play an important role, with agents targeting EGFR mutations (e.g. afatinib, erlotinib, osimertinib), *KRAS* G12C mutations (e.g. sotorasib), or *BRAF* V600E mutations (e.g. dabrafenib), among others (National Comprehensive Cancer Network, 2024). Depending on the involvement of organs in patients with extensive disease, other approaches are used additionally for local disease control or palliation, such as radiation for brain and bone metastasis, or localized therapy for qualified liver lesions (National Comprehensive Cancer Network, 2024). Despite efforts to improve treatment options for NSCLC patients, outcomes are still poor, with the 5-year overall survival ranging from 68% in stage IB to 0-10% in stage IVA-B (Duma, Santana-Davila, & Molina, 2019).

## 1.2 BCL-2 family

### 1.2.1 BCL-2 family and the apoptotic pathway

The process of apoptosis, or programmed cell death, is a crucial process that allows for proper functioning of an organism through removal of damaged, superfluous, or malfunctioning cells (Cory, Huang, & Adams, 2003). The extrinsic apoptotic pathway occurs in response to ligand engagement of cell surface death receptors, while the intrinsic (or mitochondrial) apoptotic pathway results from stressors such as growth factor withdrawal, DNA damage or oncogene activation (Campbell & Tait, 2018). This intrinsic pathway is critically regulated by the BCL-2 family of proteins, which comprises both pro- and anti-apoptotic members, and which are categorized into three subgroups (Cory, Huang, & Adams, 2003). All member proteins contain a BH3-domain, one of four different BH domains, which facilitate their interactions (Fig. 3A) (Kale, Osterlund, & Andrews, 2018). When an apoptotic signal is transmitted along the pathway, it activates the pro-apoptotic proteins BAX and BAK, which oligomerize and permeabilize the mitochondrial outer membrane through pore formation. This causes the release of caspase-activating proteins and other cell death mediators from the intermembrane space. The caspases cleave many proteins that are necessary for normal cell function and homeostasis, ultimately leading to initiation of death (Fig. 3B) (Cory, Huang, & Adams, 2003; Kale, Osterlund, & Andrews, 2018; Yip & Reed, 2008). The second group, termed BH3-only proteins, includes e.g. BIM, BAD or BIK, and facilitates this process by binding to the BH3-domain binding groove in BAX and BAK, thereby activating them. On the other hand, the pro-survival family members, such as BCL-2, can bind to the former two groups and thereby inhibit apoptosis (Kale, Osterlund, & Andrews, 2018). The balance of pro- and anti-apoptotic proteins can be affected by many stimuli, such as nutrient deprivation or presence of DNA damage, which then decides the cell's fate (Warren, Wong-Brown, & Bowden, 2019).

Intriguingly, some of the BCL-2 family members have also been shown to have functions outside of the apoptotic pathway. The anti-apoptotic protein BCL-xL, for example, has been proposed to impact the efficiency of energy metabolism through regulation of ATP synthesis (Alavian et al., 2011). BAD has been proposed to affect glucose homeostasis both through interacting with the enzyme glucokinase, as well as through its impact on insulin secretion (Danial et al., 2003; Danial et al., 2008). The pro-apoptotic BAK has been shown to have an additional function in regulating

neuronal activity, e.g. through altering neurotransmitter release (Fannjiang et al., 2003). As previously stated, multiple BCL-2 family members have also been shown to regulate endoplasmic reticulum (ER) calcium homeostasis through binding to different 1,4,5-trisphosphate receptors (IP<sub>3</sub>-receptors), which are crucial for multiple signaling pathways (Gross & Katz, 2017).

**Anti-apoptotic:**



**Pro-apoptotic:**



**Figure 3A. Comparison of BCL-2 family proteins.** All proteins have at least one BCL-2 homology (BH) domain (BH1, BH2, BH3, or BH4) and typically also have a transmembrane domain (TM). (Some BH3-only proteins do not have a TM; dashed line). Adapted from Yip & Reed, 2008.

### 1.2.2 BCL-2 family and cancer

Given that the ability to resist apoptosis has long been postulated as one of the hallmarks of cancer development (Hanahan & Weinberg, 2000), the involvement of BCL-2 family proteins as regulators of this process has long been investigated. BCL-2 was the first family member to be implicated in carcinogenesis, specifically in B-cell lymphomas, where a translocation between chromosomes 14 and 18 leads to increased *BCL-2* transcription and therefore pro-survival signaling (Warren, Wong-Brown, & Bowden, 2019). Inactivating frameshift mutations in the *BAX* gene have been found in about 50% of colon cancers with microsatellite instability, resulting in decreased cancer cell death (Rampino et al., 1997). Overexpression of the anti-apoptotic member *MCL-1* has been found in both solid and hematologic malignancies (Tantawy et al., 2023), and in our own group we confirmed dependence of cancer cells on MCL-1 in lung cancer models (Munkhbaatar et al., 2020). The intrinsic functions of BCL-2 family members likely also explain, why these proteins have been linked to chemotherapy-resistance in patients, as well as prognostic significance in leukemia patients receiving traditional cytotoxic agents (Yip & Reed, 2008). In

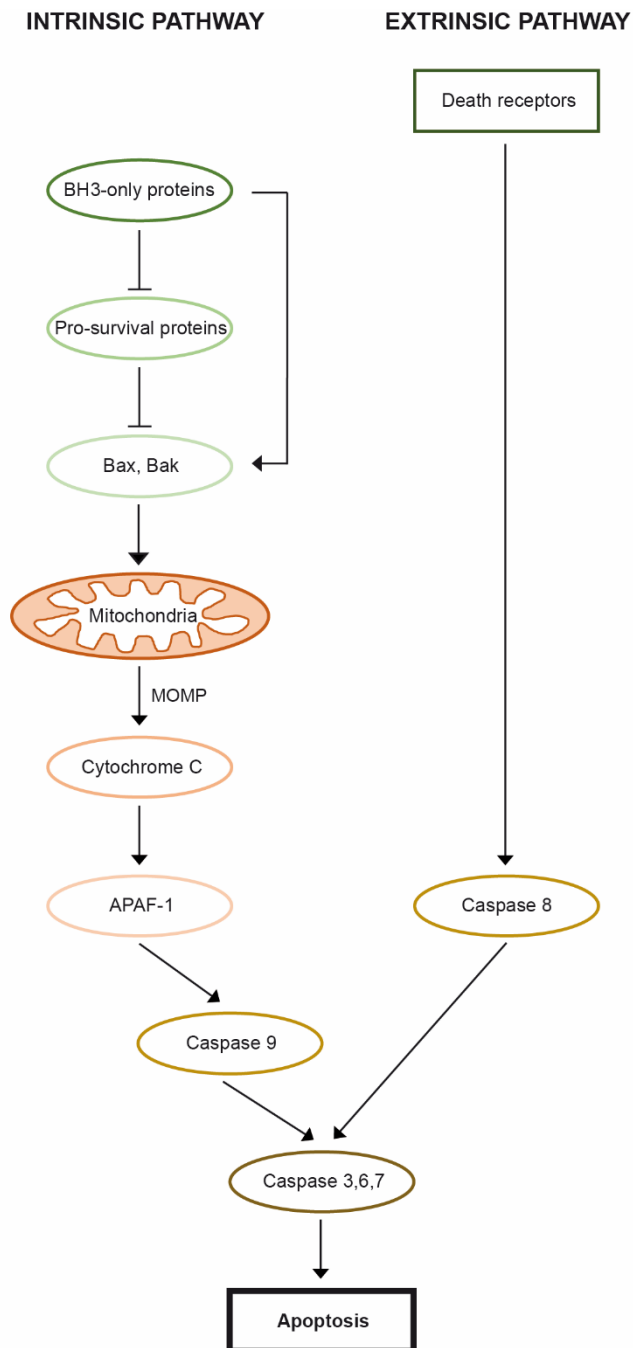


**Figure 3B. The BCL-2 family regulates the apoptotic signaling pathway.** Various stimuli, including oncogenic stress or intracellular damage, initiate the intrinsic apoptotic pathway. The activated BH3-only proteins inhibit of the pro-survival BCL-2 family members. This induces activation of BAX and BAK, causing mitochondrial outer membrane permeabilization (MOMP) and cytochrome C release. Alternatively, BH3-only proteins can directly activate BAX and BAK. Cytochrome C release induces caspase 9 activation in a complex with APAF-1, leading to activation of the effector caspases 3, 6 and 7. The extrinsic pathway is induced by binding of ligands to their respective death receptors. This results in caspase 8 activation, which can engage both the intrinsic and extrinsic pathways. Both

pathways converge at the level of activated caspase 3, which finally causes apoptosis. Adapted from Cory, Huang, & Adams, 2003 and Campbell & Tait, 2018.

order to target these key roles in cancer cells, multiple targeted agents have now been developed. Most notably, the BCL-2-specific BH3 mimetic ABT-199 (Venetoclax) is now widely used in treating chronic lymphocytic leukemia (CLL) and being studied in other entities. Multiple BH3 mimetics targeting MCL-1 have also been developed and their efficacy is being tested in clinical trials (Campbell & Tait, 2018).

### 1.3 BCL-2 related ovarian killer “BOK”

The BCL-2 family member BOK (BCL-2-related ovarian killer) was first identified in ovarian cells using MCL-1 as bait in a yeast two-hybrid screen (Hsu et al., 1997). BOK was assigned to the pro-apoptotic multi-BH-domain subfamily due to its sequence homology to BAX and BAK (73% and 87%, respectively) (Echeverry et al., 2013).

The first *Bok*<sup>-/-</sup> mouse model was published in 2012 (Ke et al., 2012). These BOK-deficient mice did not exhibit an overt phenotype, which was confirmed by two independently generated models (Carpio et al., 2015; Llambi et al., 2016). When gene knockout of BOK was added to BAX- or BAK deficient animals (*Bok*<sup>-/-</sup>*Bak*<sup>-/-</sup> and *Bok*<sup>-/-</sup>*Bax*<sup>-/-</sup>), this addition did not dramatically exacerbate the preexisting single knockout phenotypes (Ke et al., 2013). Upon evaluation of the hematopoietic system, triple-knockout animals (*Bok*<sup>-/-</sup>*Bax*<sup>-/-</sup> *Bak*<sup>-/-</sup>) did show a more severe phenotype, such as with increased lymphoid infiltration of organs, leading authors to postulate a redundant function of BOK within the hematopoietic system (Ke et al., 2015).

On a cellular level, BOK was initially felt to also be a bona fide MOMP mediator (Zheng et al., 2018), like BAX and BAK (Llambi et al., 2016). In contrast to BAX and BAK, however, BOK also localizes to the Golgi apparatus, and more prominently to the endoplasmic reticulum (Echeverry et al., 2013), where it interacts with IP<sub>3</sub>-receptors (Schulman et al., 2013). There, its activity is negatively regulated by ER-associated degradation (Llambi et al., 2016). The first experiments showed induction of apoptosis upon over-expression of BOK in cell lines (Hsu et al., 1997). This was mirrored in human tissue samples, where it was shown that BOK expression was associated with elevated trophoblast cell death in placental tissue from women with preeclampsia (Ray et al., 2010; Soleymanlou et al., 2005). However, subsequent data indicated that the absence of *Bok* can decrease cellular proliferation, e.g. in a mouse model of hepatocellular carcinoma

(HCC), where it promoted HCC development (Rabachini et al., 2018), pointing rather to an anti-apoptotic role. A connection of BOK to ER stress has also been examined, and findings proposed BOK activity to be negatively regulated by ER-associated degradation (Llambi et al., 2016) and that it is a critical inducer of apoptosis in response to ER stress (Carpio et al., 2015). Of note, the latter findings were disputed by another group, who argue that BOK is not essential in promoting ER-stress induced apoptosis in the model of *Bok*-deficiency that they separately generated (Fernandez-Marrero et al., 2016), thus adding to the uncertainty around the function of this protein. Srivastava et al. suggested that BOK interacts with the UMP synthase enzyme, aiding its function in nucleotide synthesis and thus promoting cellular proliferation and chemosensitivity (Srivastava et al., 2019). BOK has also been linked to the pathway of p53-mediated cellular response to DNA damage, with Zhang et al showing increased levels of damage in the absence of BOK (Yakovlev et al., 2004; Zhang et al., 2019). It has been postulated, that the differing results obtained by different groups are due to *Bok* being investigated in an “exogenous” (or cell-free) versus “endogenous” context, in which it is not free but rather sequestered to the ER by IP<sub>3</sub> receptors (Bonzerato & Wojcikiewicz, 2023). Others further propose that the localization of BOK within the cell, whether to the ER membrane, the mitochondria or the nucleus, accounts for its different effects (Naim & Kaufmann, 2020).

While its function and purpose have remained, in part elusive, Beroukhim et al. found that the genomic locus containing *BOK* (amongst several other genes) is frequently deleted in a wide-ranging screen of human cancer samples and cell lines, containing multiple different cancer entities (Beroukhim et al., 2010). While this locus contained multiple genes, *BOK* was favored to be the most likely target of this deletion. This was by them interpreted as pointing towards a previously unknown function of BOK as a tumor suppressor, thus underlining the need for further investigation.

#### **1.4 Mouse models of lung cancer**

Multiple different murine models of lung cancer have been developed and are now employed in varying research settings. In order to yield the most accurate information and provide relevant insights into human lung cancer, a mouse model should closely resemble the initiation and progression of cancer as it occurs in humans. This will also yield the most applicable results in treatment experiments.

Carcinogen-based mouse models use cancer-inducing chemicals to produce physiologically relevant changes in the lung parenchyma and thereby facilitate tumor development (Fig. 4B) (Hynds et al., 2021). These models typically use strains of mice that are more susceptible to spontaneous tumor development, such as A/J or SWR mice (Meuwissen & Berns, 2005). Tobacco-derivatives, such as nitrosamines (e.g. N-nitroso-tris-chloroethyl urea (NTCU)) and polycyclic hydrocarbons (benzo[a]pyrene, 3-methylcholanthrene (MCA)), or urethane (which is found in fermented foods and beverages) are highly effective carcinogens that are commonly used and mimic the toxins that humans are exposed to (Hynds et al., 2021; Meuwissen & Berns, 2005). Benefits of using chemical carcinogens include high reproducibility and efficacy of inducing adenomas or adenocarcinomas (Meuwissen & Berns, 2005). An even more accurate model of human lung cancer, however, can be generated using transgenic mouse models.

Genetically engineered mouse models (GEMMs) are mouse strains that have been genetically altered to express certain oncogenes or delete specific tumor suppressors, which enables tumor development (Fig. 4A) (Kwon & Berns, 2013). While generation of GEMMs previously took a substantial amount of time, the development of CRISPR-Cas9 genome editing accelerated this process (Hynds et al., 2021). Most of the available models have focused on adenocarcinoma, and with the discovery of driver mutations in human cancers, these mutations have become the basis to generate GEMMs (Meuwissen & Berns, 2005). While strains harboring EGFR mutations, EML4-ALK fusions or ROS1 fusions are available, the most commonly used mice harbor *Kras* variants (Hynds et al., 2021). Specifically the conditional *Lox-Stop-Lox-Kras<sup>G12D</sup>* mouse has been widely used. Here, tumors are induced by exposing mice to Adeno-Cre or Lenti-Cre viruses and thereby allowing for activation of the nascent oncogene (Jackson et al., 2001; Meuwissen & Berns, 2005). Sporadic virus-induced activation of mutated *Kras* in individual cells, that are in an environment otherwise made up of normal cells, closely mimics human tumorigenesis (Jackson et al., 2001).

### **1.5 Aims of this project**

It has long been known how important apoptosis and the BCL-2 family are in cancer development. Despite years of research, however, there is still much to learn about this family, and some its members, specifically BOK, remain elusive. In their screen of many types of human cancer,

A

Genetically engineered mouse models				
	Mouse mutant	Tumor induction	Histologic Phenotype	Reference
	LSL-Kras <sup>G12D</sup>	Sporadic infection of lung cells with AdenoCre virus	Adenomas, adenocarcinomas	Jackson et al., 2001
	Kras <sup>G12D</sup> LA1 and LA2 in WT or p53 deficiency	Spontaneous lung tumor development due to sporadic switching of LA allele	Adenomas, adenocarcinomas	Johnson et al., 2001
	Tet-op-Kras <sup>G12D</sup> in WT or p53 and P19Arf deficiency	CCSP-rtTA transgene, treatment with doxycycline	Adenomas, adenocarcinomas	Fisher et al., 2001
	LSL-Kras <sup>G12D</sup>	Tamoxifen Cre-ERT2 knockins in SPC and CC10	Adenomas, adenocarcinomas	Xu et al., 2012
	Beta-Actin lox-GFP-lox-Kras	Ad5-CMV-Cre	Adenomas, adenocarcinomas	Meuwissen et al., 2001
	LSL-Kras <sup>G12D</sup> ;p53lox/lox	Sporadic switching of lung cells with Lenti Cre virus	Adenomas, adenocarcinomas	Winslow et al., 2011
	LSL-Kras <sup>G12D</sup> ;PTEN-lox/lox	Clara cell specific CCSP-Cre	Adenomas, adenocarcinomas	Iwanaga et al., 2008
	LSL-Kras <sup>G12D</sup> ;Lkb1lox/lox	Ad5-CMV-Cre	Adenocarcinomas, squamous cell carcinomas	Ji et al., 2007
	LSL-Kras <sup>G12Vgeo</sup>	Cre-ERT2 (RERT-ert) + Tamoxifen	Adenomas, adenocarcinomas	Guerra et al., 2003
	TRE-Egfr L858R/T790M/Del exon 19 mutants	CCSP-rtTA doxycyclin inducible	Adenocarcinomas	Politi et al., 2006; Regales et al., 2007
	Tet-op-PIK3CA H1047R; CCsp-rtTA	CCSP-rtTA doxycyclin inducible	Adenocarcinoma with bronchioalveolar features	Engelman et al., 2008

B

Carcinogen-induced models			
	Carcinogen	Histologic Phenotype	Reference
	Urethane	Kras-driven adenocarcinoma	Shimkin et al., 1975
	Benzo[a]pyrene	Squamous Lesions	Saffiotti et al., 1968
	3-methylcholanthrene (MCA)	Squamous cell carcinoma	Nettesheim et al., 1971
	N-nitroso-tris-chloroethylurea (NTCU)	Squamous cell-like lung cancer	Tago et al., 2013

**Figure 4. Overview of mouse models for NSCLC.** Some commonly used models utilize either genetically engineered mice (A) or carcinogens (B). Adapted from Hynds et al., 2021 and Kwon & Berns, 2013.

Beroukhim et al. found the locus containing *BOK* to be frequently deleted. This makes detailed characterization of the function of BOK even more important, as it could deepen our understanding of cancer, aid in finding new treatment approaches, and could even help in our understanding of other diseases, in which BOK may play a role. Lung cancer remains a common and deadly cancer diagnosis all over the world, and we now have many well-established mouse models to investigate this disease. Therefore, my aim was to elucidate the role of the BCL-2 family member BOK within the context of lung cancer.

Specifically, my aim was to study *Bok*-deficient animals in a *Kras*-inducible model of lung adenocarcinoma, both in the presence and absence of *Tp53*. I wanted to characterize differences between genotypes as well as at different time points, to mimic cancer evolution in humans. Based on the available data, I initially postulated that *Bok*-deficiency might lead to accelerated tumorigenesis, and that it might be involved in a number of different cellular functions such as apoptosis or DNA damage response. Based on the *in vivo* generated results, I would then use commercially available murine NSCLC cell lines to confirm and further characterize my findings *in vitro*.

## 2. Materials and Methods

---

### 2.1 Cell culture

The murine NSCLC cell lines LKR10 and LKR13 (lung adenocarcinoma derived, *Kras* mutated, *Tp53* wildtype) were cultured in RPMI medium 1640 (ThermoFisher Scientific, MA, USA) supplemented with 10% fetal bovine serum (FBS Good Forte, PAN-Biotech, Germany), 1% penicillin/streptomycin, and 2mM L-Glutamine (ThermoFisher Scientific). Murine embryonic fibroblasts (MEF) (from Walter and Eliza Hall Institute of Medical Research) were cultured in DMEM supplemented with 10% FBS, 50  $\mu$ M 2-mercopethanol and 1% penicillin/streptomycin. Human embryonic kidney 293T (HEK293T) cells were cultured in DMEM supplemented with 10% FBS and 1% penicillin/streptomycin. All cells were cultured at 37°C in an atmosphere containing 5% CO<sub>2</sub>. Cells were routinely checked for mycoplasma contamination.

### 2.2 Inducible BOK overexpression

The tamoxifen-inducible BOK expression vector was kindly provided by the Thomas Kaufmann lab. For transfection,  $2 \times 10^6$  HEK 293T cells were seeded the day prior, then transduced with GEV-16, BOK or eGFP using pMDL plasmid, pRSV-REV plasmid, gag/pol plasmid, env plasmid and metafectene in DMEM media. After two spin infections, selection of transduced LKR13 cells was achieved using hygromycin 150  $\mu$ g/ml and puromycin 4  $\mu$ g/ml (concentrations previously determined). Cells were then seeded at a density of  $5 \times 10^5$  cells, and the following day treated with 5 $\mu$ M 4-hydroxytamoxifen 4-OHT (previously determined to be the ideal concentration) to induce expression.

### 2.3 CRISPR/Cas9-mediated genome editing

Using CRISPR/Cas9-mediated genome editing (targeting sequence: 5'-TCCCAGCGTATAACCGAACG-3') the *Bok* gene was targeted in the murine lung adenocarcinoma cell line LKR10. Targeting guides were cloned in the px458 plasmid, which also carries a GFP expressing cassette (pSpCas9(BB)-2A-GFP (PX458) was a gift from Feng Zhang, Addgene plasmid # 48138; <http://n2t.net/addgene:48138>; RRID:Addgene\_48138). LKR10 cells were transfected with the *Bok*-targeting plasmid and the *LacZ* control using Metafectene®

(Biontix Laboratories, Germany). GFP positive cells were single sorted using BD FACSAria Fusion flow cytometer (BD Biosciences) to generate new cell lines, in which successful deletion of *Bok* was detected by Western blot. The newly generated LKR10 *Bok*<sup>-/-</sup> and LKR10 *LacZ* cells were maintained in medium as detailed above.

## 2.4 Immunoblotting

One day prior to cell lysate preparation,  $1 \times 10^6$  cells were seeded in 10cm dishes. They were lysed using RIPA buffer (Cell signaling cat# 9806) with protease inhibitors (complete protease inhibitor cocktail, Roche). Protein concentrations were determined by BCA assay (Thermo Scientific cat# 23225) and the extracts were denatured in Laemmli loading buffer containing 5%  $\beta$ -mercaptoethanol. This was followed by separation via SDS-PAGE and transfer onto nitrocellulose membranes. Antibodies used were BOK (1:1000, Abcam, ab233072, clone BOK-R1-5-1); BOK (1:200, clone 1–5, provided by T. Kaufmann and already validated in Echeverry et al., 2013); MCL-1 (1:1000, Bundoora Mab lab, clone# 19C4-15); cleaved caspase 3 (1:1000, Cell signaling, cat# 9662);  $\beta$ -actin (1:1000, Cell Signaling, cat #4970, clone #13E5).

## 2.5 Quantitative real-time PCR (qPCR)

After cell harvest, RNA was collected and purified using the NucleoSpin RNA kit (Macherey-Nagel, cat# 740955.50) according to manufacturer instructions. The RNA concentration and its purity were measured using the NanoDrop spectrophotometer (NanoDrop Technologies). cDNA was then synthesized from 1  $\mu$ g RNA by using SuperScript II Reverse Transcriptase (Invitrogen, cat# 18064-014) according to the manufacturer's protocol. The quantitative PCR was performed using LightCycler 480 (Roche) Real-Time PCR System with the provided protocol. *Bok* expression was normalized to the reference gene expression. Primers used were as follows: *Bok*: for 5'-TTCATGCCCTGGTTGACTGCCT, rev 5'-AAGCCAGGATCTGTGCTGACCA; *HPRT1*: for 5'-GCTGACCTGCTGGATTACAT, rev 5'-TTGGGGCTGTACTGCTTAAC.

## 2.6 Cell proliferation and viability analysis

For cell proliferation analysis, 3,000 cells per line were plated in 96-well plates in triplicates and were counted by Trypan Blue exclusion after 48h, 72h, and 96h. For cell cycle analysis, cells were collected and fixed in 70% ethanol, followed by Ribonuclease A treatment (RNase A, ThermoFisher Scientific), and propidium iodide staining (PI, Sigma-Aldrich, MO, USA). Data

were acquired by the BD FACSCanto (BD Biosciences) and then analyzed using the Watson pragmatic algorithm available in the FlowJo software (v. 9.7.6, BD Biosciences) or ModFit LT 5.0 (ModFit LT). Cells for treatment with chemotherapeutic agents were seeded the day prior at a density of 5,000 cells per well in a 96 well plate. After treatment with the cytostatic agents, the viability was determined using the CellTiter-Glo Luminescent Cell Viability Assay (Promega) according to the manufacturer's instructions at 24h, 48h, and 72h timepoints.

## 2.7 Comet assay

Cells were seeded in 10 cm dishes at a density of  $1.5 \times 10^6$  the day prior to the experiment and then treated with Etoposide (6  $\mu\text{g/ml}$ ) at 37 °C for 3h or 8h. The cells were harvested, resuspended in ice-cold PBS at  $1.4 \times 10^5$ , and then prepared using the Trevigen CometAssay Kit according to the manufacturer's protocol. The cells were then combined with low-melting agarose at a ratio of 1:10 and spread onto the CometSlides. Gelling was achieved in the dark at 4 °C for 10 min, slides were subsequently placed in 4 °C Lysis Solution overnight. After incubating the slides in alkaline unwinding solution for 20 min at room temperature (200 mM NaOH, 1 mM EDTA), electrophoresis was done at 4 °C and 1 V/cm in alkaline electrophoresis solution (200 mM NaOH, 1 mM EDTA) for 25 min. The slides were dried at 37 °C and DNA was stained in the dark using propidium iodide (1 mg/ml stock solution) at a 1:1500 dilution for 15 min. Slides were analyzed using the OpenComet software tool (<https://cometbio.org/index.html>).

## 2.8 Mouse strains

Previously established *Lox-Stop-Lox-Kras<sup>G12D/+</sup>* (*LSL-Kras<sup>G12D/+</sup>*) mice (Jackson et al., 2001) were crossed with *Bok<sup>-/-</sup>* mice (generated on a C57BL/6 genetic background) (Ke et al., 2012) to generate mice of the following three genotypes: *LSL-Kras<sup>G12D/+</sup> Bok<sup>-/-</sup>*, *LSL-Kras<sup>G12D/+</sup> Bok<sup>+/-</sup>*, and *LSL-Kras<sup>G12D/+</sup> Bok<sup>+/+</sup>*. In a second set of experiments, these mice were backcrossed on a *Tp53<sup>fl/fl</sup>* background (Marino et al., 2000) to generate: *LSL-Kras<sup>G12D/+</sup> Bok<sup>-/-</sup> Tp53<sup>fl/fl</sup>*, *LSL-Kras<sup>G12D/+</sup> Bok<sup>+/-</sup> Tp53<sup>fl/fl</sup>*, and *LSL-Kras<sup>G12D/+</sup> Bok<sup>+/+</sup> Tp53<sup>fl/fl</sup>* animals. Mice were maintained in pathogen-free conditions with free access to food and water.

## 2.9 Tumor induction

Mice of the above genotypes from the same litters were used as age matched controls. At age 6-8 weeks the animals were anesthetized with a mixture of medetomidine (0.5 mg/kg), midazolam (5

mg/kg) and fentanyl (0.05 mg/kg) (MMF) based on their weight. They were then intranasally infected with  $5 \times 10^6$  PFU of adenovirus expressing Cre recombinase, as previously described (Munkhbaatar et al., 2020), via two instillations of 62.5 $\mu$ L at 4 minutes apart (virus provided by Dr. Martina Anton, Institut für Experimentelle Onkologie und Therapieforchung, MRI, TUM). All animal experiments were approved by and conducted in accordance with the District Government of Upper Bavaria (AZ: 55.2-1-54-2532-55-12).

## **2.10 Tissue harvesting**

Mice were sacrificed at the indicated timepoints of either 19 or 29 weeks. The trachea was exposed during necropsy and the lungs inflated with air prior to removal. The organs were fixed in 4% paraformaldehyde at room temperature for 24 hours and then transferred to 70% ethanol and given for dehydration. The lobes were then placed into histological cassettes in a fixed pattern and embedded in paraffin.

## **2.11 H&E staining and tumor burden analysis**

To quantify the tumor burden in the lung tissue after 19 or 29 weeks, the formalin fixed paraffin embedded (FFPE) lungs were cut into three-step sections at 100  $\mu$ m intervals to yield slides of 2  $\mu$ m thickness. One 2  $\mu$ m slide from each step section was stained with hematoxylin and eosin (H&E) and scanned with a SCN400 slide scanner (Leica Biosystems). For tumor burden analysis, three slides per animal, each 100  $\mu$ m apart, were evaluated and both the lobe and individual lesion areas were defined manually and measured using the Aperio ImageScope software (version 12.4, Leica Biosystems). The total area of the lesions was normalized over the total area of the lung for each slide. The average of three analyzed H&E slides was used for the reported data. This analysis was done with the experimenter blinded to genotype. For tumor grading, the slides were given to a pathologist for blinded evaluation and lesions were classified as hyperplasia, atypical adenomatous hyperplasia (AAH), adenoma, or adenocarcinomas, as previously described (Jackson et al., 2001).

## **2.12 AB-PAS staining**

AB-PAS staining (Alcian Blue and Periodic Acid Schiff staining) was performed on 2  $\mu$ m slides with a stain kit (cat# 38016SS5, Leica biosystems) and using the protocol provided with the kit. In brief, slides are stained using Alcian blue, Schiff's reagent and hematoxylin in multiple steps

with rinsing in between each step. The stain detects structures containing a high amount of carbohydrates such as glycoproteins or proteoglycans.

### **2.13 Immunohistochemistry (IHC)**

Immunohistochemical staining was performed using the Leica BOND RXm (Leica Biosystems, Nussloch, Germany), using a DAB-based detection system (BOND Detection System, Leica Biosystems). The following primary antibodies were used: goat polyclonal CC10 (sc-9772, Santa Cruz Biotechnology, TX, USA), goat polyclonal SP-C (sc-7705, Santa Cruz Biotechnology, TX, USA), mouse monoclonal Ki-67 (cat. #550609, BD Biosciences, NJ, USA), rabbit polyclonal cleaved caspase-3 (Cell Signaling Technology, MA, USA), rabbit monoclonal Phospho-Ser139-Histone H2AX ( $\gamma$ -H2AX, cat. #9718, Cell Signaling Technology, MA, USA), rabbit monoclonal CD3 (cat# RM-9107S0, LabVision/NeoMarkers Corporation, CA, USA), rat monoclonal CD45R/B220 (cat# 55084, BD Biosciences, NJ, USA), and rat monoclonal F4/80 (cat# T-2006, BMA Biomedicals AG, Augst, Switzerland). All stained sections were acquired with the SCN400 slide scanner (Leica Biosystem) and analyzed by experimenter blinded to genotype. For the analysis of Ki67 and  $\gamma$ -H2AX IHC stains, the six most advanced lesions on each slide were evaluated by software-based analysis using the Positive Pixel Count v9 algorithm available in the Aperio ImageScope software (version 12.4, Leica Biosystems) and the resulting data was normalized to lesion area. Other stains were analyzed manually with the experimenter blinded to genotype.

### **2.14 Absorption-based X-ray micro-CT**

Lungs that had previously been air-inflated and fixed in formalin were stored in 70% ethanol, and then prior to imaging were stained with 1% iodine (I<sub>2</sub>) dissolved in absolute ethanol (I2E). The lungs were then placed in fixed position in an ethanol-filled tube and measured with absorption-based micro-CT (versaXRM-500 from Zeiss Xradia). These experiments and reconstructions were performed in collaboration with Pidassa Bidola and Kirsten Taphorn (IMETUM / Chair of Biomedical Physics (E17), TUM).

### **2.15 Seahorse assay**

The day prior to the experiment, 30,000 cells, which was the previously determined optimal cell density, were seeded into a Seahorse XF Cell Culture Microplate (Agilent Seahorse XF Cell Mito

Stress Test Kit, Agilent, CA, USA). The experiment was then performed according to the manufacturer's protocol, using the agents oligomycin, carbonyl cyanide-4 (trifluoromethoxy) phenylhydrazone (FCCP) and a rotenone/antimycin A mixture. Through titration experiments, these were determined to be the optimal concentrations: 1 $\mu$ M oligomycin, 2 $\mu$ M FCCP, 10 $\mu$ M rotenone. Each experiment was performed in eight replicates and using the Agilent Seahorse XF Analyzer device. Parameters were then calculated by the Seahorse XF Mito Stress Test Report Generator.

### **2.16 TCGA data analysis**

The data set TCGA\_LUAD\_exp\_HiSeqV2-2015-02-24 was downloaded from the website of the UCSC Cancer Browser (<https://genome-cancer.ucsc.edu/>). This data set contained 511 total lung adenocarcinoma samples, as well as 57 tumor samples with paired healthy lung tissue. Files named "genomic Matrix" in these datasets were used to obtain levels of mRNA expression. The RSEM normalized mRNA count (Li & Dewey, 2011) represents TCGA mRNA expression, the unit for gene expression being  $\log_2(\text{count}+1)$ . This was done in collaboration with Xin Wang.

### **2.17 Statistical analysis**

The details of experiments, including sample number, statistical tests used, and dispersion and precision measures, are stated in the figures or figure legends. The data analysis was performed with GraphPad Prism 5.0 software. The appropriate statistical test was selected depending on data type and distribution. For all statistical tests statistical significance was determined if the p value was less than 0.05.

## 3. Results

---

### 3.1 BOK levels in human lung cancer samples

The impetus for this project being Beroukhim et al.'s finding that the locus containing BOK was frequently deleted in human tissue samples and cell lines, I sought to reproduce this using the publicly available TCGA data set TCGA\_LUAD\_exp\_HiSeqV2-2015-02-24. Comparing the BOK expression of the paired samples, we found that expression levels in tumor lesions were decreased at a statistically significant level compared to the paired healthy samples (Fig. 5A). Interestingly, the range of expression levels between the tumor samples was very broad, indicating heterogeneous genotypes between patients and calling into question whether this finding can be assigned clinical significance. When comparing the BOK expression levels of patients stratified by TNM stage, lymph node status or smoking history, there was no difference seen (Fig. 5B). While not a direct part of this dissertation, our group worked with collaborators using the TRACERx dataset. Interestingly, it was seen clearly that *BOK* was not significantly deleted on a gene level in LUAD patients (Meinhardt et al., 2022). These discrepancies have to further be seen in context with prior descriptions of a lack of correlation between BOK mRNA and protein levels. Taken together, it remains to be conclusively understood in what way the absence of BOK, whether on a gene, mRNA or protein level, is relevant in human patients.

### 3.2 In vitro overexpression of BOK

Next, I sought to explore the role of BOK in cell survival, and whether it truly is pro-apoptotic as initially proposed, in a controlled in vitro setting. Many of the initial findings with regards to BOK were obtained through models of overexpression in cell lines, so I attempted to replicate this in the lung cancer setting. The murine lung adenocarcinoma cell line LKR13 was used and transduced with a Tamoxifen-inducible Bok overexpression vector, a GFP vector was used as positive control. At the end of the experiment, successful expression of GFP in the control cells could be visualized through fluorescence microscopy (data not shown) and through immunoblotting (Fig. 6A). On further examination, the Bok vector-containing cells, when expression was induced with Tamoxifen, were found to have a slight increase in the Bok RNA levels via quantitative PCR (Fig. 6B). There was no clear difference, however, between BOK protein levels of either cell type (Fig.

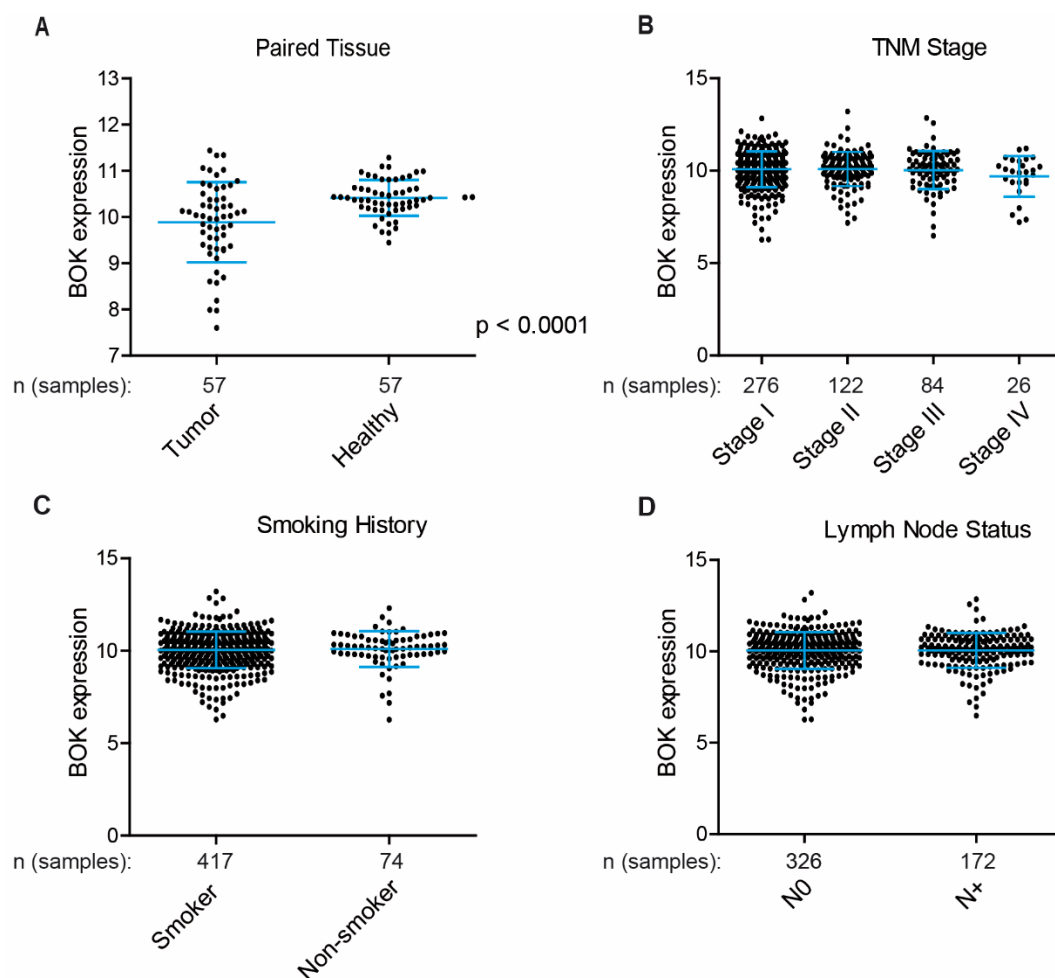


**Figure 5. BOK expression in human lung cancer samples.** Using a TCGA dataset, BOK expression was determined in 511 lung adenocarcinoma samples, including 57 with paired healthy lung tissue (A). There was no significant difference in BOK expression levels when stratifying patients based on their TNM stage (B), their smoking history (the smoker category includes both current and former smokers) (C) and lymph node involvement (N0: none, N+: some degree of involvement) (D). Data analyzed by paired t-test, one-way ANOVA and unpaired t-test with Welch correction, respectively.

6A). Fittingly there was no difference in levels of cleaved caspase 3, or the well-established interaction partner MCL-1 (Fig. 6A). This is in line with previous publications describing discrepancies between BOK mRNA and protein levels *in vitro* and proposing that these may, at least in part, be due to high BOK protein turnover (Llambi et al., 2016; Moravcikova et al., 2017). In our setting of murine LUAD cell lines, we were unable to reproduce the BOK overexpression-induced cell death seen by others.

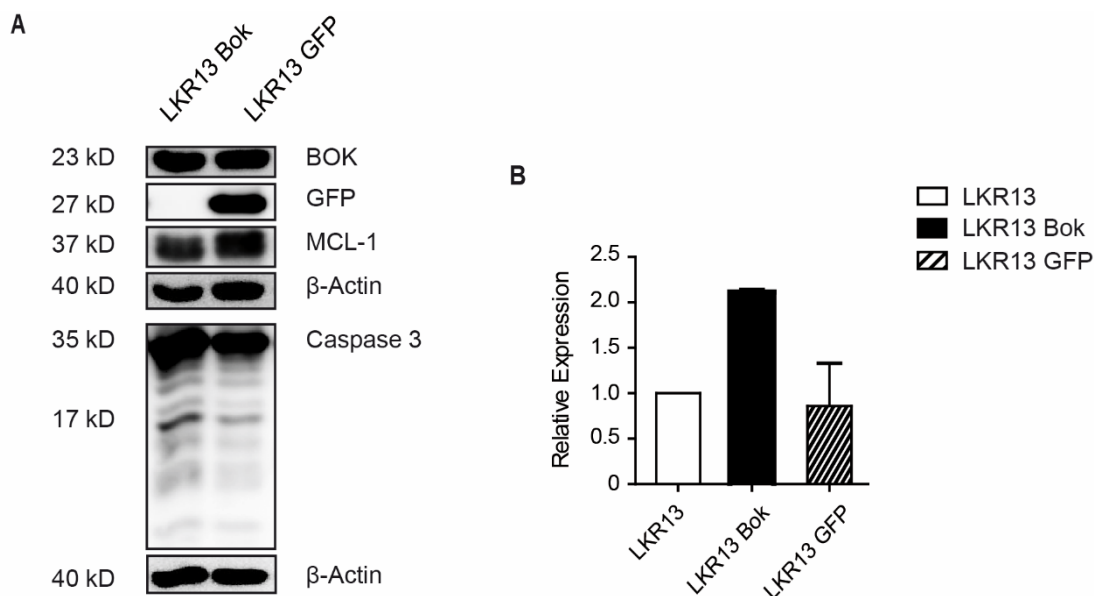


**Figure 6. Inducible BOK overexpression.** (A) Immunoblotting of murine lung cancer cell line LKR13 transduced with the inducible BOK overexpression vector (LKR13 Bok) or GFP (LKR13 GFP) to detect BOK, GFP, MCL-1 and (cleaved) caspase 3. (B) Relative expression of BOK determined by quantitative PCR using triplicates of the former cell lines as well as untreated cells (LKR13). All cells were treated with 5 $\mu$ M tamoxifen to induce expression.

### 3.3 BOK-deficient cell lines show decreased proliferation

Given the question of whether our overexpression model can yield relevant results, we pursued another experimental setting to determine the role of BOK in survival and/or apoptosis. I used CRISPR/Cas9-mediated genome editing on the murine lung adenocarcinoma-derived cell line LKR10 to generate BOK-deficient cell lines (LKR10 *Bok*<sup>-/-</sup>). *LacZ* was used as a control (LKR10 *lacZ*) (Fig. 7A). To determine any baseline proliferative differences, I determined absolute cell numbers over time (at 24 hours, 48 hours, 72 hours) while cells were kept in culture and at ideal conditions. Intriguingly, I found that BOK-deficient cells, even without an extrinsic stimulus, proliferate more slowly than the controls (Fig. 7B). This has also been described in other cell types (Srivastava et al., 2019). By doing a cell cycle analysis via flow cytometry, I could also show that *Bok*<sup>-/-</sup> cells show longer G2 phase duration than the *Bok*<sup>+/+</sup> cells, suggesting presence of continued DNA damage (Fig. 7C).

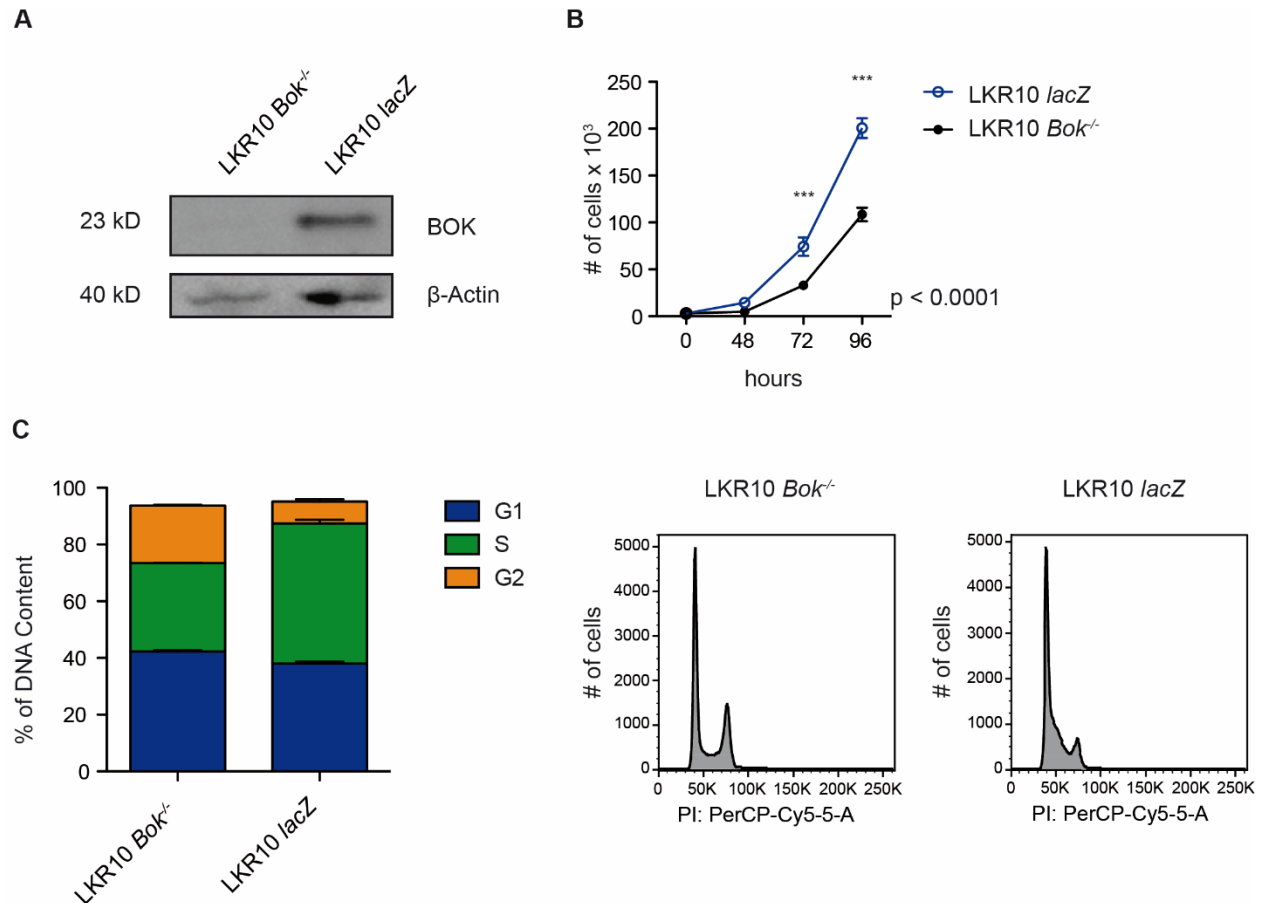


**Figure 7. BOK-deficient cells show decreased proliferation in vitro.** (A) Immunostaining of LKR10 cells confirming successful deletion of *Bok* in LKR10 cell line (compared to *lacZ* control cells). (B) Live cell numbers evaluated by trypan blue exclusion over time. Data are presented as mean  $\pm$  SEM and were analyzed by repeated measure two-way ANOVA (time, genotype, and interaction effects,  $p < 0.0001$ ). Post hoc analysis with Bonferroni correction showed a significant difference between the genotypes at 72h and 96h (\*\*\*:  $p < 0.0001$ ). Adapted from Meinhardt et al., 2022.

### 3.4 BOK may have an influence on cellular metabolism

Given the differences previously seen between BOK-deficient and wildtype cell lines, I chose to look for a BOK-dependent effect on the cells' energy metabolism. Using the agents oligomycin (a complex V inhibitor), carbonyl cyanide-4 (trifluoromethoxy) phenylhydrazone FCCP (an uncoupling agent, that disrupts the mitochondrial membrane potential) and a rotenone/antimycin A mixture (complex I and III inhibitor, respectively) with the Agilent Seahorse XF Analyzer, I sought to measure key parameters of mitochondrial function (Mito Stress Test). I evaluated basal respiration, which is the oxygen consumption required to meet the ATP-demand from the mitochondrial proton leak, ATP-linked respiration, which is the mitochondrial-produced ATP that

contributes to meeting the cell's energetic needs, and maximal respiration, which is the maximum rate of respiration a cell can achieve.

The BOK-proficient *lacZ* cells had higher baseline respiration than *Bok*<sup>-/-</sup>, which can indicate a higher energy demand of cells under basal conditions. Addition of oligomycin showed greater response in BOK-proficient cells, with cells having a higher proportion of basal respiration that is not coupled to ATP-synthesis (Fig. 8B). This represents the proton leak, and can indicate mitochondrial damage. Upon addition of FCCP the mitochondrial membrane should depolarize, leading to maximal proton leak and maximal respiration of the cell. Despite titration to determine the optimal FCCP concentration, which can inversely also suppress respiration if concentrations are too high, it is unclear why maximal respiration remained lower than basal respiration in these LKR10 cells. While we were not able to draw definitive conclusions from this experiment, an effect of BOK on energy metabolism remains likely.

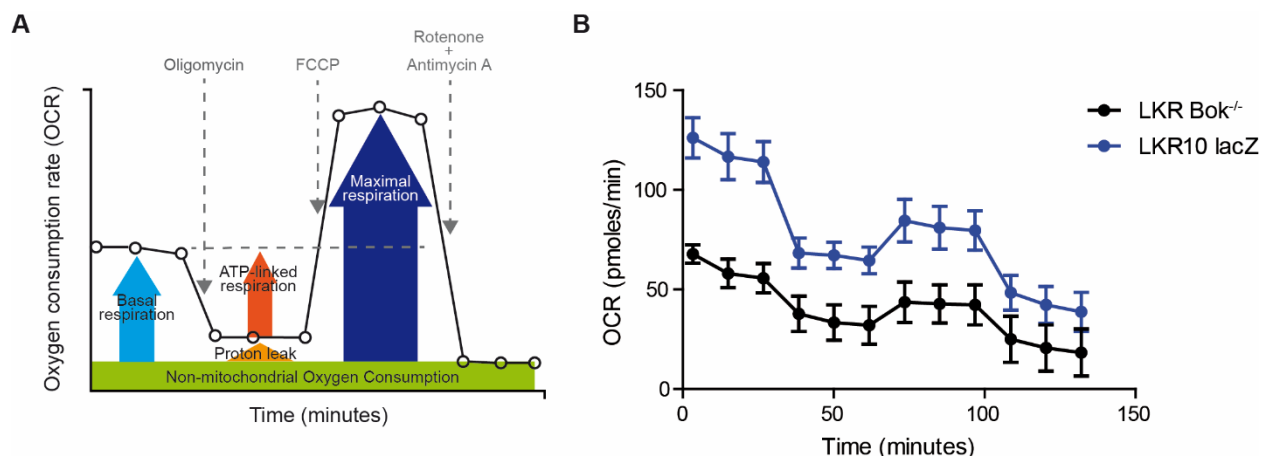


**Figure 8. BOK-dependent influence on oxygen consumption.** (A) Schematic illustration of the oxygen consumption rate determined via mito stress test on the Seahorse XF Analyzer. (B) Oxygen consumption rate of lung adenocarcinoma cell lines from a representative experiment done in quadruplicates.

### 3.5 BOK-deficiency leads to increased DNA damage in cell lines

I then sought to characterize these cells' response to stress and whether this is altered by the absence of BOK. I treated the cells with cytostatic agents that inhibit DNA topoisomerases (Etoposide and Irinotecan) or an anti-metabolite (5-fluorouracil (5-FU)). By these mechanisms, the agents induce DNA damage and are used therapeutically in many cancer types. While both cell

lines were susceptible to these agents, the presence of BOK correlated with higher viability at 24, 48 or 72 hours (Fig. 9A). BOK-deficient cells, conversely, showed a lower rate of survival in response to these DNA insults, further pointing to a role of BOK in the cellular response to DNA damage. Upon treatment with cytotoxic agents that have different mechanisms of action, such as the antimicrotubule agent Paclitaxel or the proteasome inhibitor MG-132, I saw no difference in survival between the cell lines (Fig. 9B).

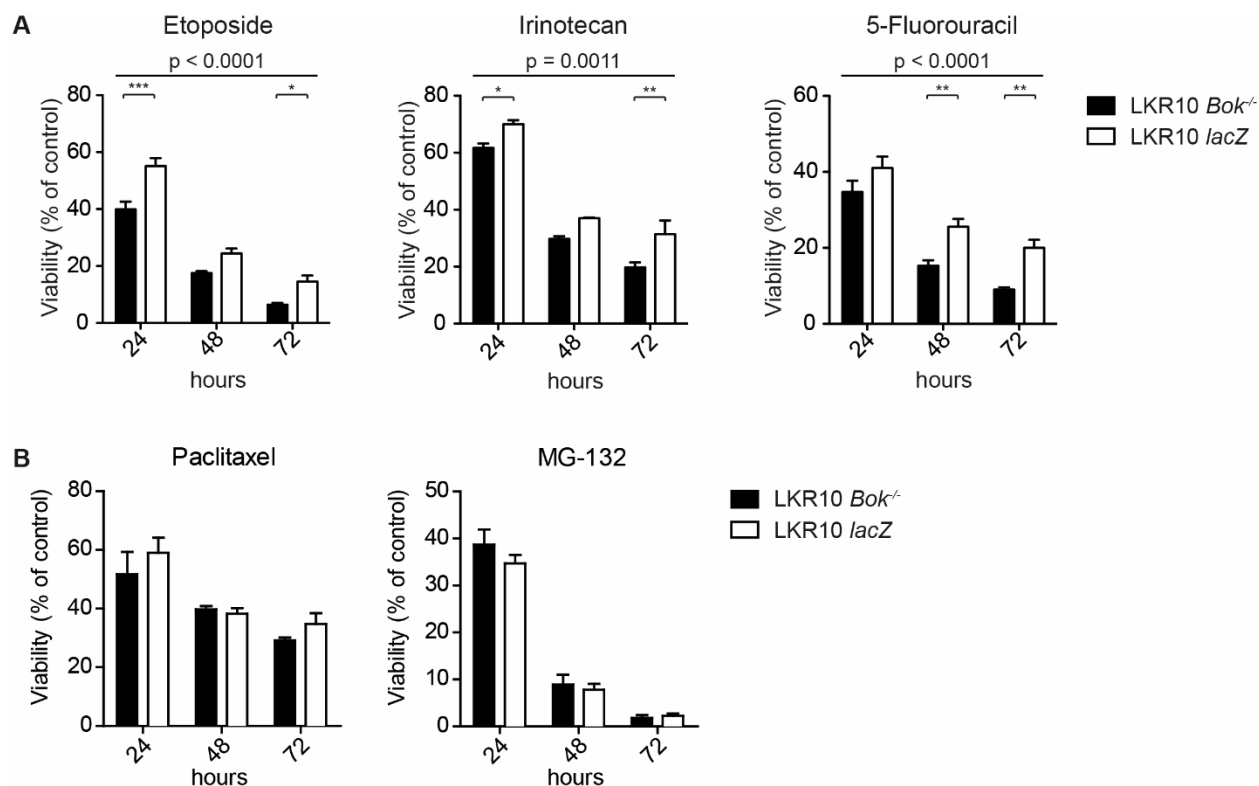


**Figure 9. BOK-deficiency sensitizes against DNA damaging agents.** LKR10 *Bok*<sup>-/-</sup> and *lacZ* cells were treated with (A) Etoposide (4 $\mu$ g/ml), Irinotecan (80 $\mu$ M), or 5-Fluorouracil (50 $\mu$ g/ml); or with (B) Paclitaxel (6 $\mu$ g/ml) or MG-132 (0.5 $\mu$ M). Cell viability was determined at the indicated times. Data are means  $\pm$  SEM of three independent experiments. Significant differences between cell lines were revealed by two-way ANOVA, Bonferroni's multiple comparison test. (\*:  $p < 0.05$ , \*\*:  $p < 0.01$ , \*\*\*:  $p < 0.001$ )

These cell lines were also analyzed via comet assay, a single cell electrophoresis that can show the presence of DNA strand breaks by fluorescence microscopy. Analyzing standard parameters such as percent DNA in the tail, tail moment, and olive tail moment, I found that after 8 hours of treatment with Etoposide, BOK-deficient cells indeed showed a higher level of DNA damage

compared to their wildtype controls (Fig. 10A and B). Altogether, this indicates that BOK may play a role in cellular response to the stress caused by DNA damage.

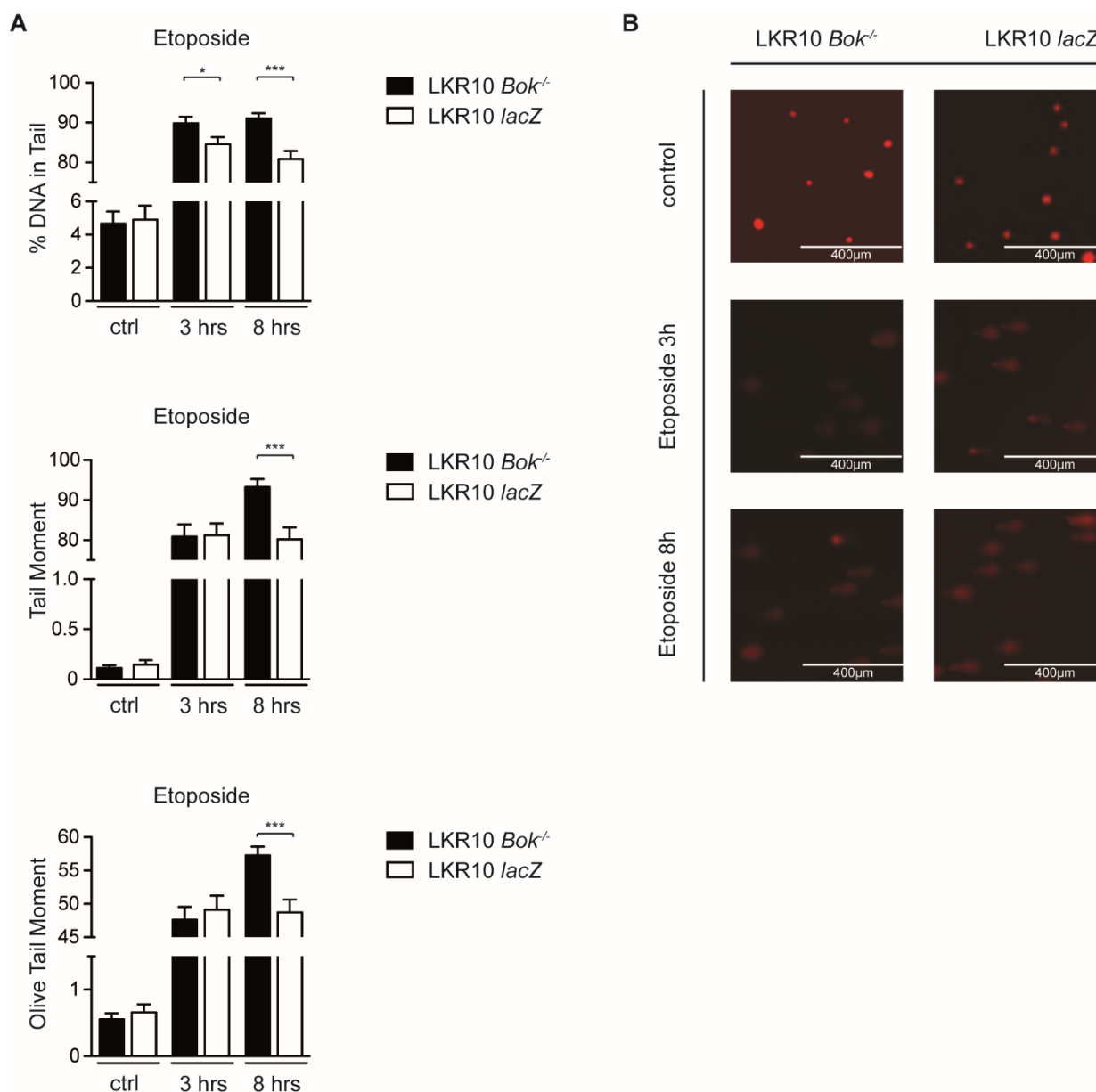


**Figure 10. BOK-deficiency leads to increased DNA damage in cells.** Cells were treated with 6µg/ml Etoposide for the indicated times and the level of DNA damage was determined by alkaline comet assay (parameters investigated were % DNA in Tail, Tail Moment, Olive Tail Moment) (A). Data are means  $\pm$  SEM of at least 25 cells per group analyzed across two slides. Statistical differences at the indicated times were determined by unpaired t-test with Welch correction (\*:  $P < 0.05$ , \*\*\*:  $P < 0.001$ ). (B) Representative microscopic images of the comet assay. Adapted from Meinhardt et al., 2022.

### 3.6 Generation of *Kras*<sup>G12D</sup>-driven lung cancer mouse model

Choosing a mouse model that closely mimics human disease under physiologic conditions is important in order to gain clinically relevant insights. To analyze the role of BOK in vivo, I used the previously discussed and well-established model with a conditionally inducible *Lox-Stop-Lox Kras*<sup>G12D</sup> allele (*LSL-Kras*<sup>G12D/+</sup> on a C57BL/6 background) (Jackson et al., 2001). In these animals, the mutated *Kras* gene is silenced by a STOP cassette, which itself is flanked by loxP sites. Upon expression of Cre recombinase in the cell, the STOP cassette is deleted, which enables expression of the oncogenic *Kras* allele and therefore controlled tumor initiation. We intercrossed these animals with *Bok*<sup>-/-</sup> animals, to generate the following genotypes: *LSL-Kras*<sup>G12D/+</sup> *Bok*<sup>+/-</sup> and *LSL-Kras*<sup>G12D/+</sup> *Bok*<sup>-/-</sup>, as well as *LSL-Kras*<sup>G12D/+</sup> *Bok*<sup>+/+</sup> as control (Fig. 11A). To achieve simultaneous and targeted expression of mutated *Kras* in the lung, we used intranasal administration of recombinant viral particles to deliver Cre expression (AdenoCre) (Fig. 11B).

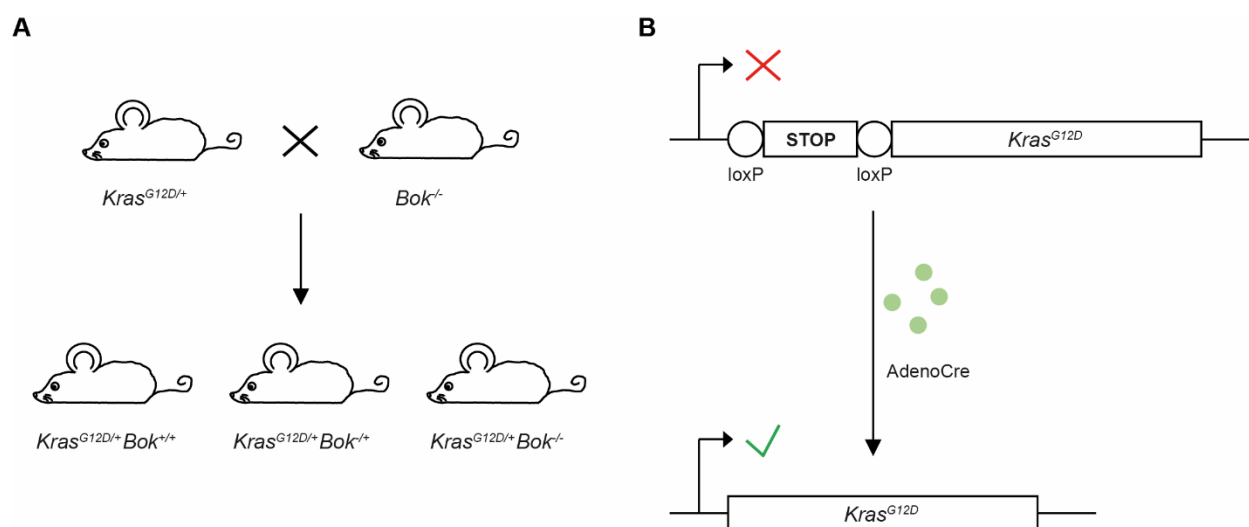


**Figure 11. Generation of *Kras*<sup>G12D</sup>-driven lung cancer mouse model.** (A) Schematic diagram of the generation of *LSL-Kras*<sup>G12D/+</sup> *Bok*<sup>+/-</sup> and *LSL-Kras*<sup>G12D/+</sup> *Bok*<sup>-/-</sup> animals through breeding. (B) Illustration of the initiation of tumorigenesis through AdenoCre-mediated deletion of the STOP cassette.

### 3.7 Characterization of BOK in *Kras*<sup>G12D</sup>-driven tumorigenesis

To determine the effect of the presence or absence of BOK on tumor development and growth, each of the three mouse cohorts were infected at an age of 6-8 weeks with  $5 \times 10^6$  PFU of AdenoCre by intranasal instillation and sacrificed after 19 weeks. Animals at this time point appeared well,

remained active and without weight loss or respiratory symptoms. On gross examination, the lungs of all three genotypes exhibited no signs of structural lung damage, and only rarely had macroscopically visible tumors (Fig. 12A). On H&E staining of lung sections, each slide revealed multiple lesions, with histological subtypes ranging from hyperplasia to (rarely) adenocarcinoma. Lesions showed characteristic malignant cellular features such as prominent nucleoli, nuclear hyperchromatism and pleomorphism.

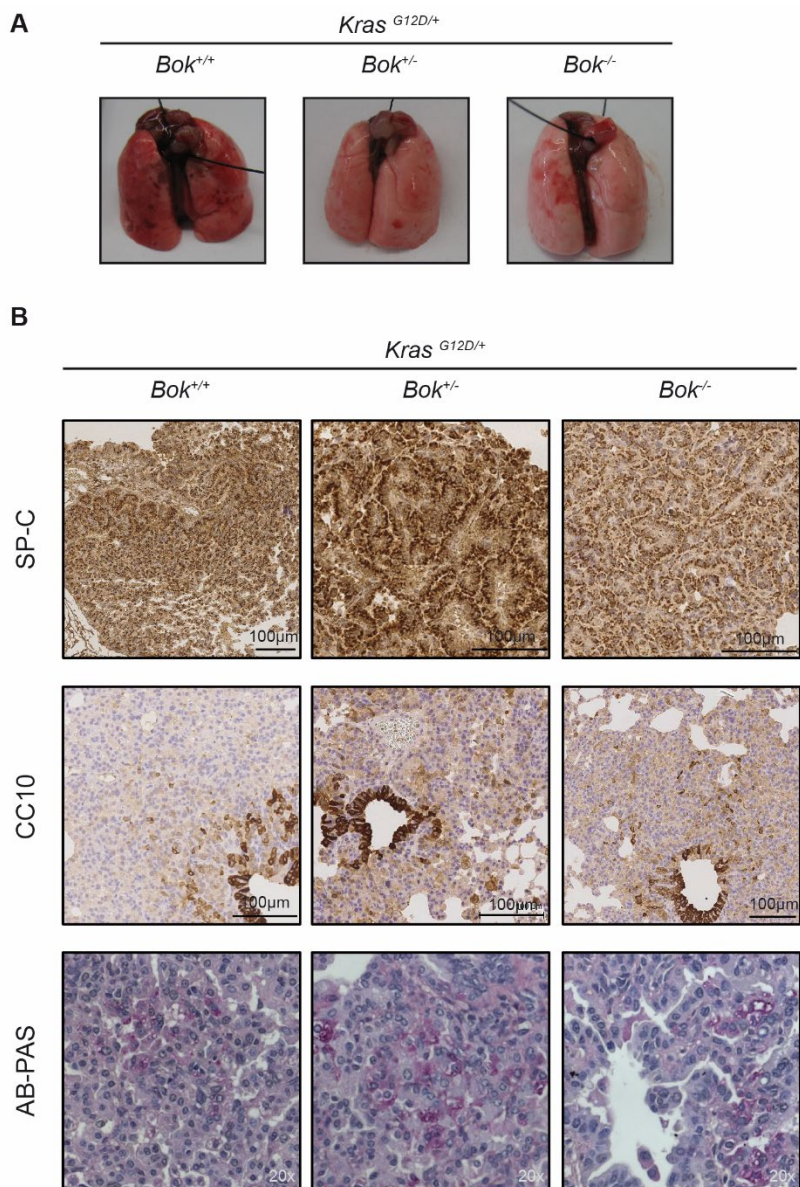


**Figure 12. Characterization of *Kras*<sup>G12D</sup>-inducible tumorigenesis.** (A) Representative lungs of the indicated genotypes 19 weeks after infection with AdenoCre without visible lung damage or tumors.

(B) Representative images depicting SP-C, CC10 and AB-PAS staining of lungs after 19 weeks of tumorigenesis.

The cell of origin for the lesions was investigated by performing immunohistochemistry (IHC) with markers for Clara cells and type II pneumocytes. In all three genotypes, the lesions were found to stain positive for the surfactant protein (SP-C), which is a surrogate marker for type II pneumocytes (Fig. 12B). Only rarely did cells stain positive for Clara cell antigen (CC10) (Fig. 12B). These stains indicate that lesions arise more likely from alveolar type II cells, or their precursors, which is consistent with previously published data and defines them as primary lung lesions (Jackson et al., 2001).

To verify the histological subtype, we performed AB-PAS staining to detect the presence of mucin, a marker of adenocarcinoma (Travis et al., 2013). All genotypes were shown to have mucin production within their tumors (Fig. 12B), confirming the subtype of adenocarcinoma and its precursor lesions.

Taken together, this data confirms the presence of pulmonary adenocarcinoma and indicates that this phenotype is not dependent on the presence of BOK.

### 3.8 BOK-deletion decreases tumor burden after 19 weeks of tumorigenesis

To investigate the role of BOK in *Kras*-driven tumorigenesis, I utilized animals of all three genotypes: *LSL-Kras<sup>G12D/+</sup> Bok<sup>+/-</sup>* and *LSL-Kras<sup>G12D/+</sup> Bok<sup>-/-</sup>*, as well as *LSL-Kras<sup>G12D/+</sup> Bok<sup>+/+</sup>* as control. After administration of AdenoCre to mice of 6-8 weeks of age, they were sacrificed after 19 weeks of tumorigenesis and their lungs harvested for further analysis. I evaluated three H&E-stained slides per animal (each 100  $\mu$ m apart) to ensure complete characterization of the entire organ. I manually determined the total number and size of lesions per slide, and tumor area per lung lobe area. While the average size of the lesions was not statistically different between all three genotypes (Fig. 13D), the overall number of lesions was significantly lower in partially or completely BOK-deficient animals (Fig. 13C). This translated to an overall decreased tumor burden that was seen in *Kras<sup>G12D/+</sup> Bok<sup>+/-</sup>* and *Kras<sup>G12D/+</sup> Bok<sup>-/-</sup>* mice, compared to their controls (Fig. 13E). Contrary to prior publications suggesting that BOK may be a tumor suppressor, in the context of *Kras*-driven lung adenocarcinoma it may aid in or facilitate the initiation or development of tumorous lesions.

### 3.9 CT imaging of lungs confirms histologic findings

In order to characterize our lungs on a 3-dimensional scale and confirm our histologic findings, we performed CT imaging on multiple lungs prior to their processing for histology. After initial fixation in ethanol, the organs were stained with 1% iodine in absolute ethanol and scanned with absorption based micro-CT. The images were then reconstructed to generate 3-dimensional models of the lungs (Bidola et al., 2019). This demonstrated equal distribution of tumors in all lung lobes

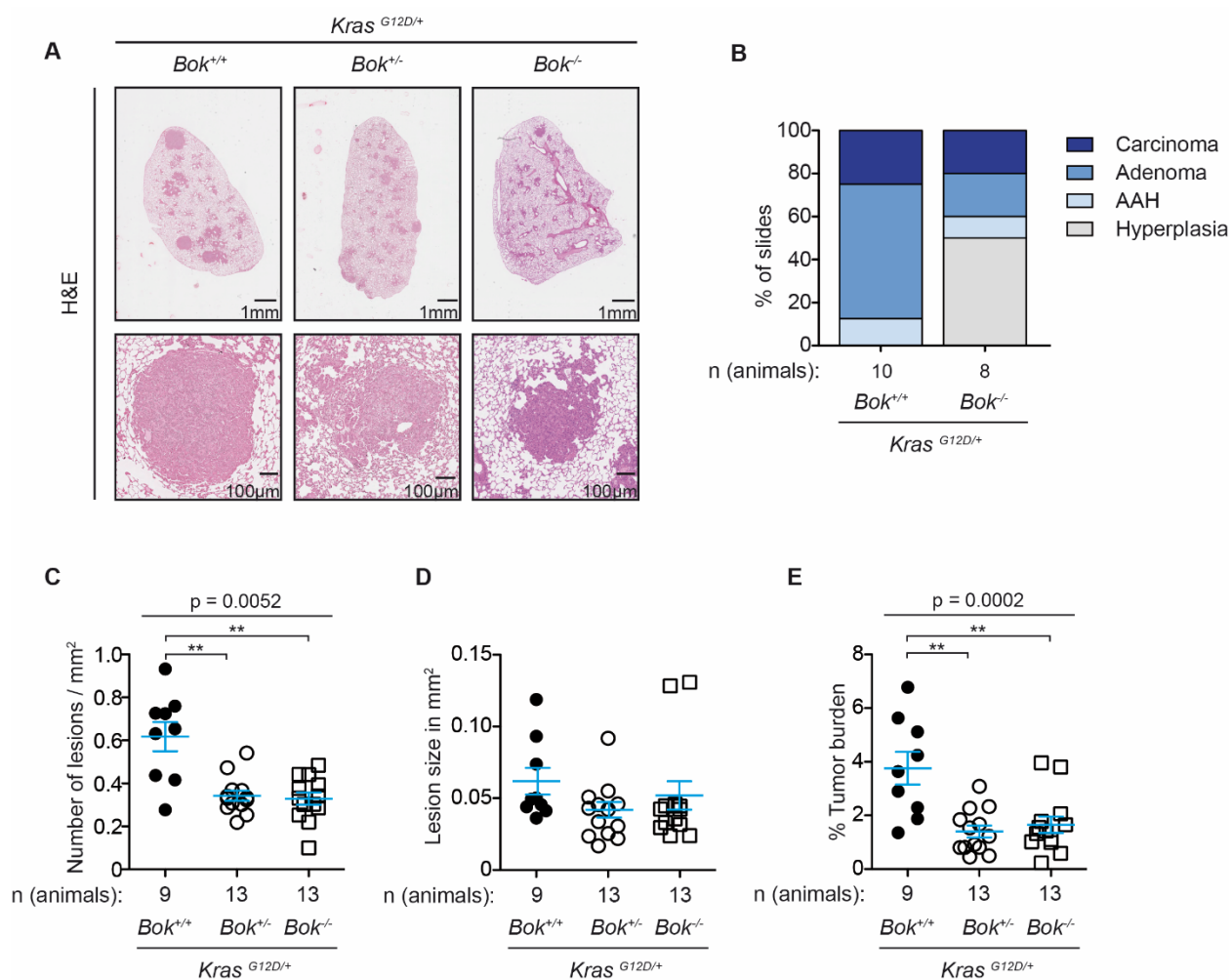


**Figure 13. BOK-deletion decreases tumor burden after 19 weeks of tumorigenesis.** (A) Representative images of H&E staining of lungs of the indicated genotypes 19 weeks after infection with AdenoCre. Bottom panels are higher magnification. (B) Percentage of slides showing at least one lesion that had advanced to the indicated histological phenotype. (C) Number of lesions per total lung area in mm<sup>2</sup>, three slides averaged per animal. (D) Lesion size in mm<sup>2</sup>, three slides averaged per animal. (E) Tumor burden calculated as tumor area (in mm<sup>2</sup>) divided by lung area (in mm<sup>2</sup>), three slides

averaged per animal. Data analyzed by unpaired two-tailed t test and one-way ANOVA with post-hoc correction. Adapted from Meinhardt et al., 2022. (\*:  $p < 0.05$ , \*\*:  $p < 0.01$ , \*\*\*:  $p < 0.001$ )

indicating sufficient spread of the liquid AdenoCre upon its administration (Fig. 14A and B). We used three  $Kras^{G12D/+}$   $Bok^{+/+}$  and three  $Kras^{G12D/+}$   $Bok^{-/-}$  lungs to calculate the overall tumor burden via CT imaging. While the absolute amounts of tumor burden were, predictably, different between the three-dimensional CT and our two-dimensional histologic analysis, we were able to show that the results generated through histology are overall representative of the organ in its entirety, and could further confirm the differences seen between the genotypes (Fig. 14C).

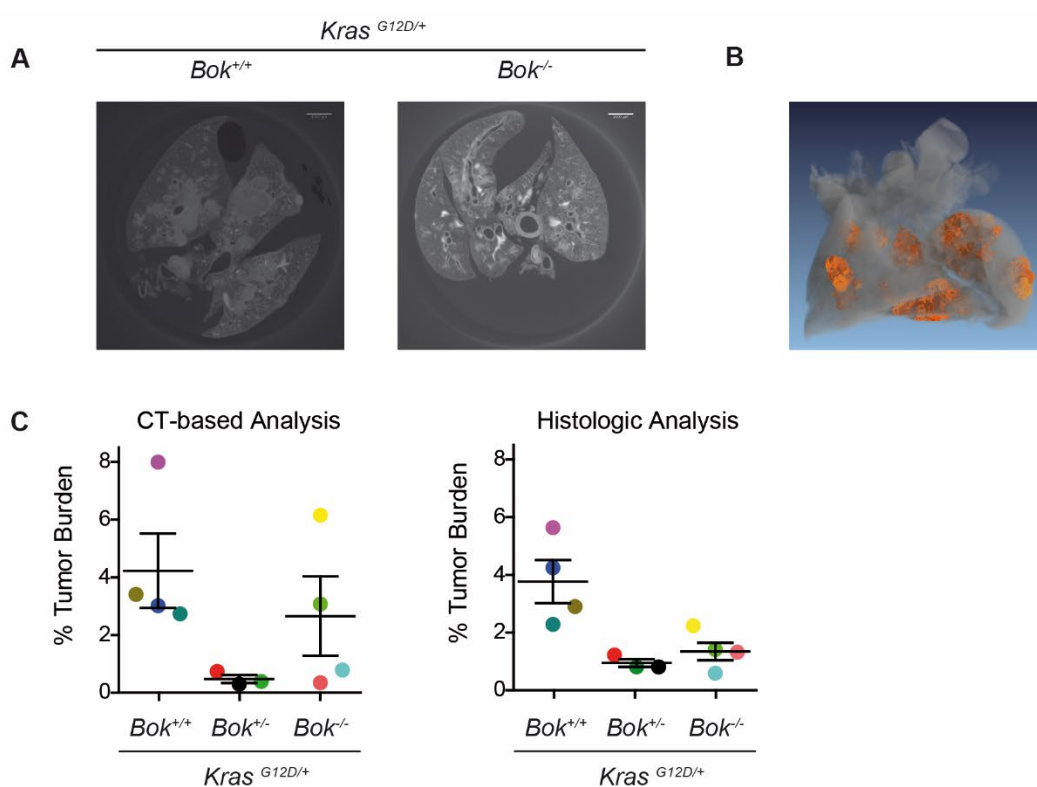


**Figure 14. CT imaging and reconstruction of murine lungs with adenocarcinoma.** (A) Representative axial plane computed tomography (CT) imaging of experimental lungs and (B) representative three-dimensional reconstruction (tumors in orange), done by Kirsten Taphorn (IMETUM). (C) Comparison of CT-based and histologic evaluation of tumor burden. Each color represents the same animal. Data presented as mean  $\pm$  SEM.

### 3.10 BOK-proficiency leads to higher tumor grades

For many cancer types, an important tool used in clinical settings is histological grading. To determine the impact of BOK-deficiency, the H&E-stained slides of our  $Bok$  wildtype and  $Bok^{-/-}$

samples were assessed based on published histological criteria (Nikitin et al., 2004). This was done in a blinded fashion in collaboration with veterinary pathologist PD Dr. med. vet. Katja Steiger (Institut für Pathologie, Technische Universität München). While early histologic stages are often not found in humans due to lack of symptoms, murine lung cancer has been shown to progress from hyperplasia to atypical adenomatous hyperplasia (AAH) to adenoma, before developing into full-blown adenocarcinomas (Jackson et al., 2001). All of these lesion types could be found in both *Kras*<sup>G12D/+</sup> *Bok*<sup>+/+</sup> and *Kras*<sup>G12D/+</sup> *Bok*<sup>-/-</sup> animals, however *Bok*<sup>-/-</sup> lesions mostly remained in early stages, while most BOK-proficient mice developed lesions in at least to the adenomatous stage (Fig. 13B). This could indicate a potential role for BOK in facilitating the initiation of *Kras*-driven lesions or help drive their progression over time.

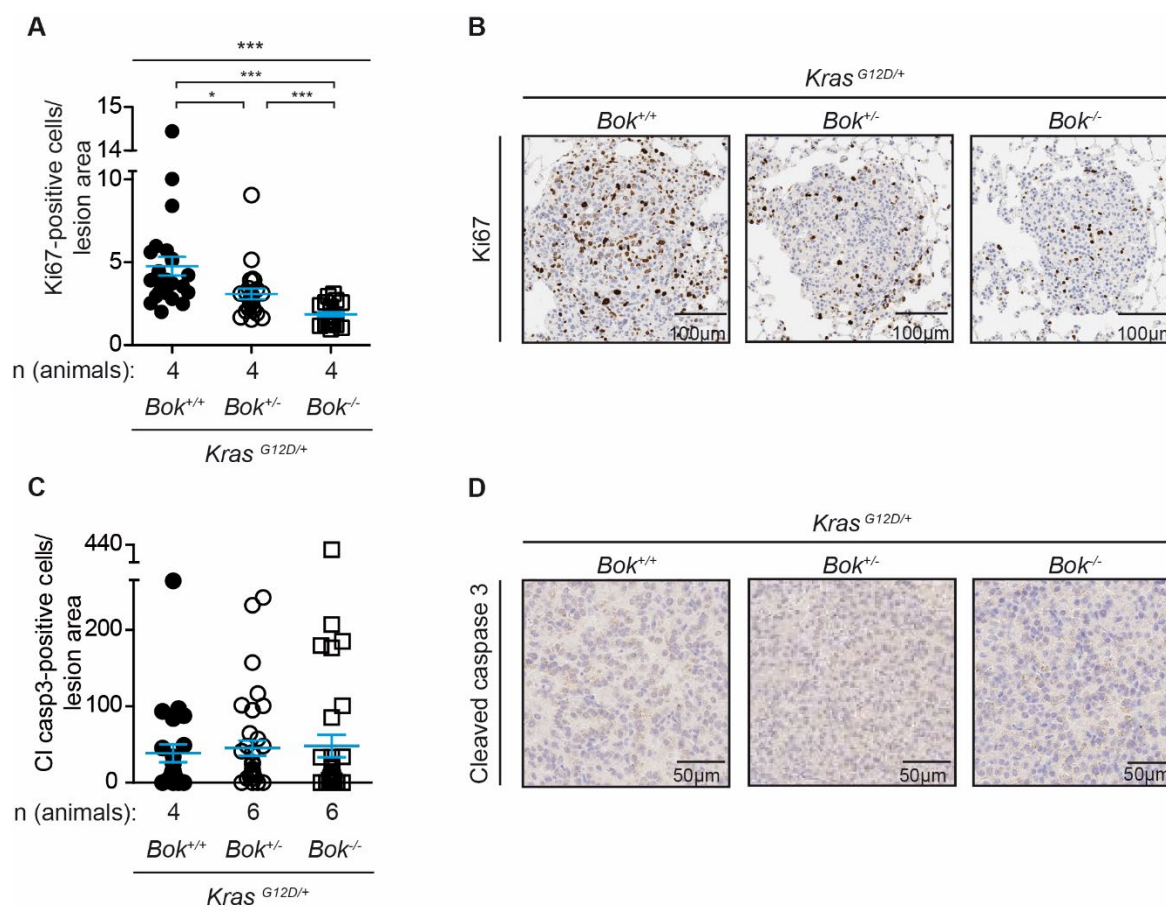


**Figure 15. BOK-deficient lesions show decreased proliferative rates.** Representative images and quantification of Ki67 staining (A, B) and cleaved caspase 3 staining (C, D). Six lesions per animal were analyzed and presented as mean  $\pm$  SEM. Data are reported as number of positive cells normalized to lesion area and analyzed by Kruskal-Wallis test with p-values from post hoc analysis. In part adapted from Meinhardt et al., 2022. (\*:  $p < 0.05$ , \*\*:  $p < 0.01$ , \*\*\*:  $p < 0.001$ )

### 3.11 BOK-deficient lesions show decreased proliferative rates

As the proliferative rate is an important characteristic of malignant lesions and BOK has been shown to impact proliferation, I analyzed Ki67 in our setting, which is a well-established immunohistochemical marker of proliferation. The expression of Ki67 is strongly associated with cell proliferation and can be detected during all active phases of the cell cycle, but not in resting cells (Scholzen & Gerdes, 2000). Consistent with prior publications in hepatocellular carcinoma (Rabachini et al., 2018), my quantitative analysis revealed that lesions expressing *Bok* showed significantly more Ki67 positive cells than *Bok*<sup>-/-</sup> lesions (Fig. 15A and B). However, I did not observe any differences in the number of apoptotic cells between *Bok*<sup>+/+</sup>, *Bok*<sup>+/-</sup> and *Bok*<sup>-/-</sup> lesions, as determined by cleaved caspase 3 staining (Fig. 15 C and D). Contrary to our initial thinking, but consistent with my in vitro data, this could indicate that BOK enables cellular proliferation.

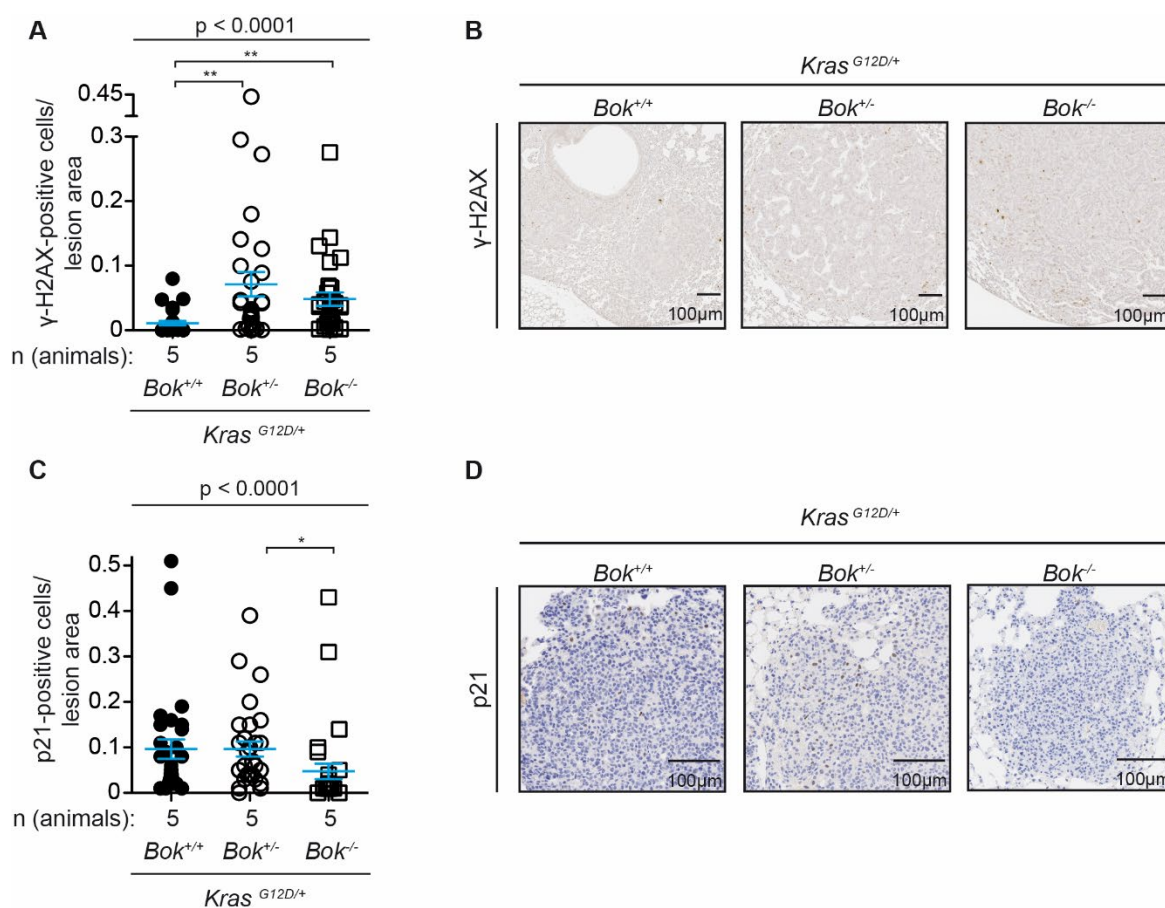


**Figure 16. BOK-deficiency leads to higher levels of DNA damage.** Representative images and quantification of  $\gamma$ -H2AX staining (A, B) and p21 staining (C, D). Six lesions per animal were analyzed and presented as mean  $\pm$  SEM. Data are reported as number of positive cells normalized to lesion

area and analyzed by Kruskal-Wallis test with p-values from post-hoc analysis. In part adapted from Meinhardt et al., 2022. (\*:  $p < 0.05$ , \*\*:  $p < 0.01$ , \*\*\*:  $p < 0.001$ )

### **3.12 More DNA damage is seen in BOK-deficient animals**

Given that my in vitro data showed evidence of increased DNA damage in BOK-deficient cells, I sought to validate this in our mouse model. To this end, I analyzed the levels of phosphorylated histone  $\gamma$ -HAX, an indicator of DNA double-strand breaks, in our experimental animals. In line with our previous findings, I detected higher levels of  $\gamma$ -H2AX in BOK-deficient lesions (Fig. 16A and B). Considering the proposed connection between the p53-pathway and BOK, I analyzed one of p53's most prominent transcriptional targets, the cyclin dependent kinase inhibitor 1A p21 (also known as p21WAF1/Cip1). Although our understanding is evolving over recent years, one of its described functions is in enabling DNA repair in response to DNA damage (Kulaberoglu, 2021). As shown in (Fig. 16 C and D), loss of BOK was associated with a decrease in the levels of the p21 protein after 19 weeks, which could contribute to the higher level of DNA damage seen. Taken together, these data show that BOK likely has an impact on DNA damage repair response, which may be linked to the p53 pathway.

### **3.13 Similar immune infiltration is seen in all genotypes**

The immune system plays an important role in cancer and can both counteract and contribute to tumorigenesis. To evaluate if the differences in tumor burden seen in our mouse model are due to an anti-tumor effect facilitated by immune cells, we performed the following IHC stains: CD3 was used to quantify T-lymphocytes, F4/80 for macrophages and CD45R/B220 to look for B-lymphocytes. Cells were seen both in the lesions themselves, as well as in the tumor periphery. As is demonstrated in Fig. 17, the total numbers of immune cells of all three subtypes were similar among the genotypes. This indicates that the decreased tumor burden in BOK-deficient animals was not mediated by an increased immune system response.

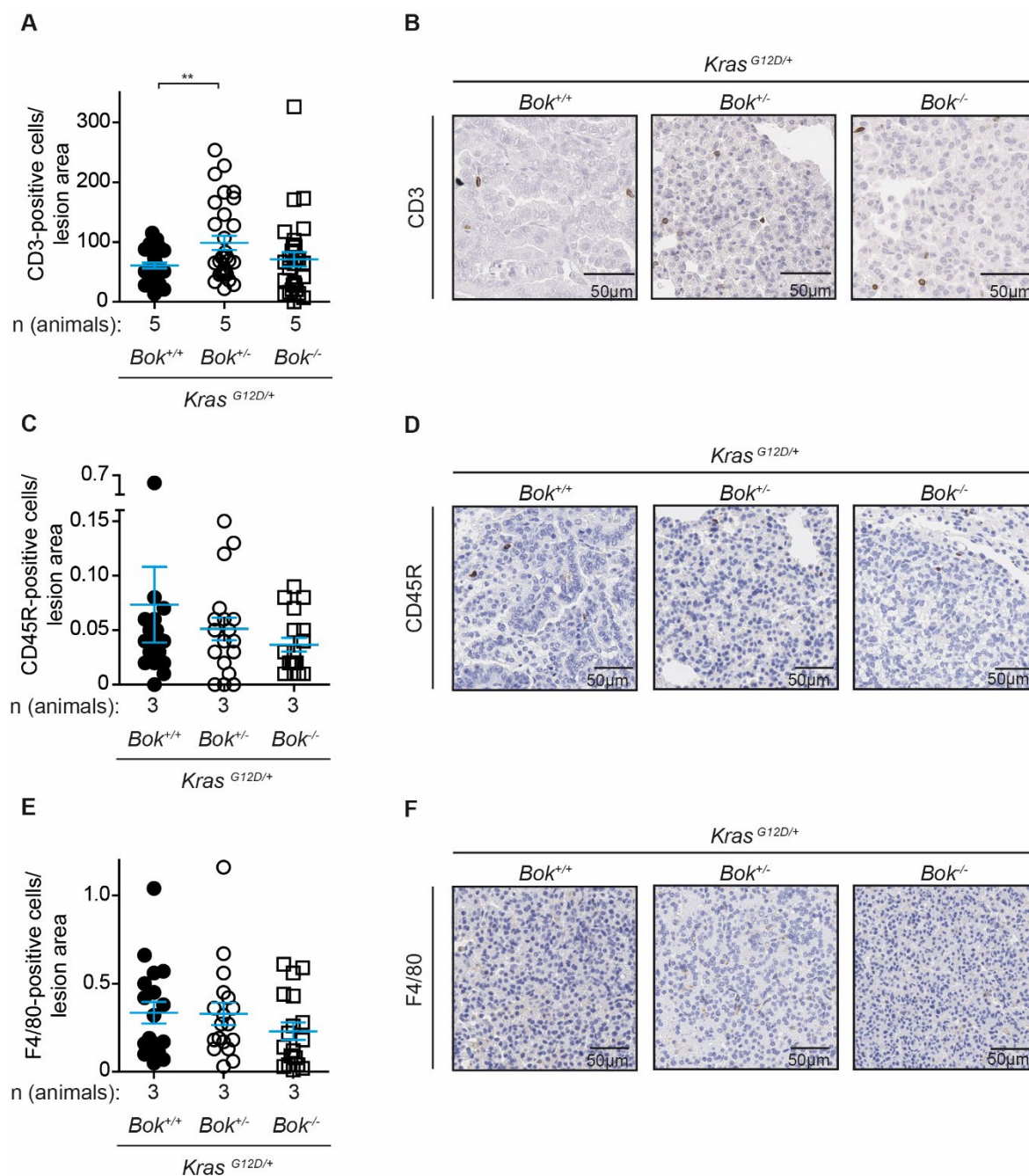


**Figure 17. Levels of immune response are independent of BOK-proficiency.** Representative images and quantification of CD3 staining for T-lymphocytes (A, B), CD45R (also known as B220) for B-lymphocytes (C, D) and F4/80 for macrophages (E, F). Six lesions per animal were analyzed and presented as mean  $\pm$  SEM. Data are reported as number of positive cells normalized to lesion area and analyzed by Kruskal-Wallis test with p-values from post hoc analysis. (\*\*:  $p < 0.01$ ).

### 3.14 Loss of phenotypic differences upon prolonged tumorigenesis

Given that only one in five animals had developed full adenocarcinomas at the 19-week timepoint, I decided to age animals to 29 weeks to enable further tumorigenesis, in an attempt to mimic the human disease even more closely. I expected to see the same pattern that was present earlier, namely with BOK-deficient lesions having a lower tumor burden. After 29 weeks however, *Bok*<sup>+/+</sup> and *Bok*<sup>-/-</sup> animals had similar tumor overall burdens (Fig. 18E). BOK-deficient animals continued to have a lower number of lesions (Fig. 18C), as was seen at 19 weeks, but the size of most lesions was now similar and some of the BOK-deficient lesions even exceeded the wildtype lesions in size (Fig. 18D). This could indicate a role for BOK in the initiation and formation of lesions, but less so in the growth of existing lesions. On the other hand, it is possible that over the prolonged aging period the lesions accumulated further genetic aberrations that may either negate or overcome the effect of BOK-deficiency.

I also pursued blinded histologic grading of the lesions, as described at the earlier timepoint. Here, I observed that almost all animals had developed at least one adenocarcinoma, confirming that additional time enables the mice in this model to develop disease similar to that of humans. Both BOK-proficient and -deficient lesions had progressed to aggressive histologic phenotypes at this timepoint (Fig. 18B), whereas *Bok*<sup>-/-</sup> animals at 19 weeks had had significantly fewer aggressive lesions.

In support of this phenotype, when looking at Ki67 positivity to evaluate for proliferation, I found that lesions from all genotypes had overall similar proliferative rates, regardless of BOK status (Fig. 18F). This contrasts with the 19-week timepoint where BOK-deficiency correlated with decreased proliferation. DNA damage, as evaluated by  $\gamma$ -H2AX IHC staining, was also similar when comparing *Bok*<sup>+/-</sup> and *Bok*<sup>-/-</sup>-animals (Fig. 18G). While heterozygous animals had a statistically higher amount of damage compared to the other genotypes, a very large distribution prohibits any conclusions at this time. Staining for p21 showed increased levels of p21-positivity in BOK-deficient cells at this late timepoint, whereas they were decreased at the early timepoint (Fig. 18H). Taken together with the previous stains, BOK-deficient cells now reached similar levels of proliferation and DNA damage as the control cells, leading to a potentially increased need for cellular response mechanisms, such as p21.

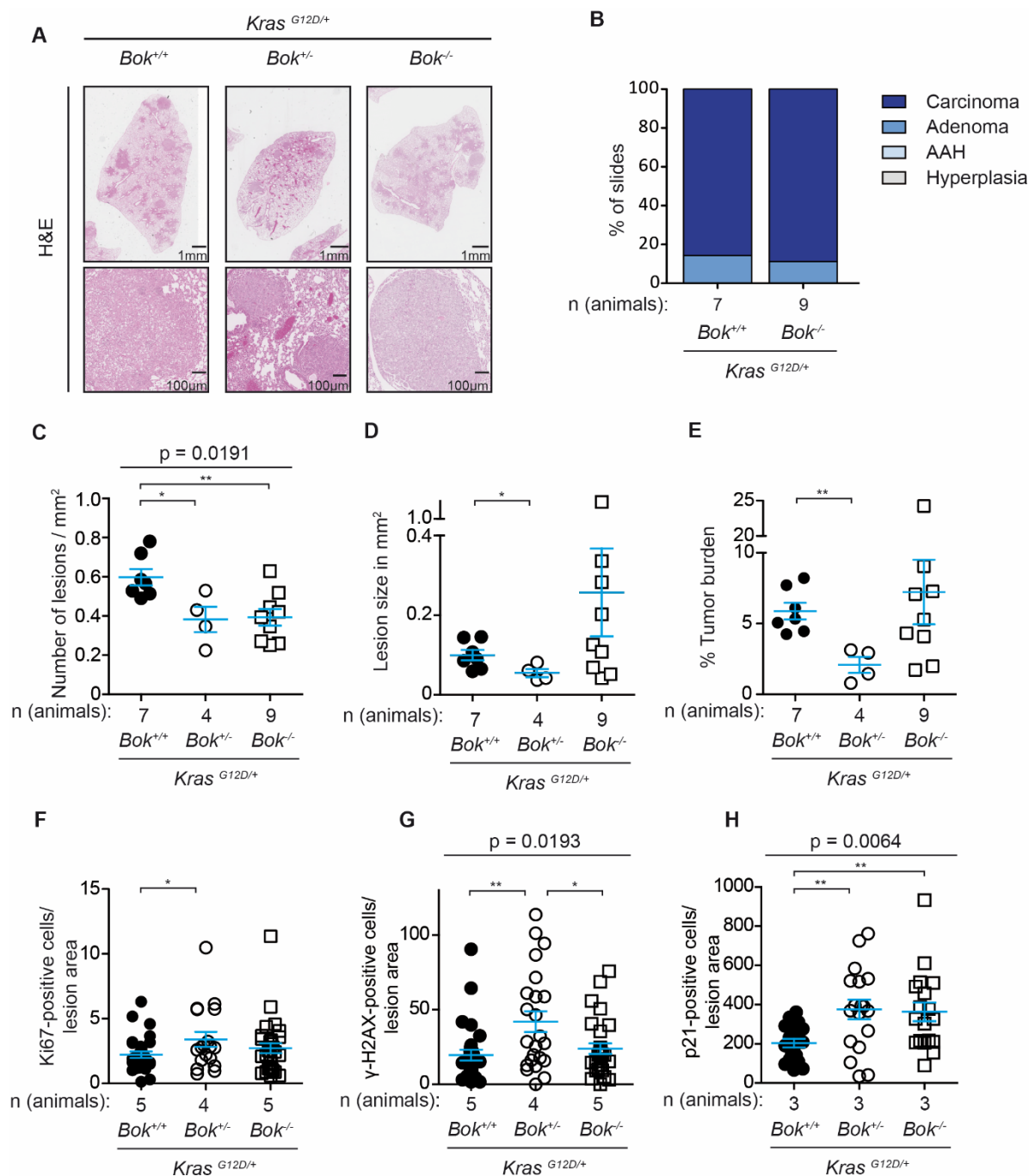


**Figure 18. Prolonged tumorigenesis of 29 weeks eliminates many BOK-dependent phenotypic differences.** (A) Representative images of H&E staining of lungs of the indicated genotypes 29 weeks after infection with AdenoCre. Bottom panels are higher magnification. (B) Percentage of slides showing at least one lesion that had advanced to the indicated histological phenotype. (C) Number of lesions per total lung area in mm<sup>2</sup>, three slides averaged per animal. (D) Average lesion size in mm<sup>2</sup>, three slides averaged per animal. (E) Tumor burden calculated as tumor area (in mm<sup>2</sup>) divided by lung area (in mm<sup>2</sup>), three slides averaged per animal. Data analyzed by unpaired two-tailed t test and one-way ANOVA with post-hoc correction. Quantification of Ki67 staining (F),  $\gamma$ -H2AX staining (G), and

p21 staining (H). Six lesions per animal were analyzed and presented as mean +/- SEM. Data are reported as number of positive cells normalized to lesion area and analyzed by Kruskal-Wallis test with p-values from post hoc analysis. (\*:  $p < 0.05$ , \*\*:  $p < 0.01$ , \*\*\*:  $p < 0.001$ )

### 3.15 Influence of co-deletion of the tumor suppressor *Tp53*

I also wanted to investigate the proposed connection of BOK to the p53 pathway in vivo, as well as enable more rapid progression of lesions to the stage of adenocarcinoma, which is the disease as it presents in humans. To this end, I generated an additional mouse strain by crossing the *LSL-Kras<sup>G12D/+</sup> Bok<sup>-/-</sup>* mice with *Tp53<sup>fl/fl</sup>* animals. This allows for simultaneous deletion of the tumor suppressor p53 with the activation of *Kras<sup>G12D</sup>* upon administration of Cre recombinase, as has been previously published (Jackson et al., 2005). The following genotypes were used: *LSL-Kras<sup>G12D/+</sup> Bok<sup>-/-</sup> Tp53<sup>fl/fl</sup>*, *LSL-Kras<sup>G12D/+</sup> Bok<sup>+/-</sup> Tp53<sup>fl/fl</sup>*, and *LSL-Kras<sup>G12D/+</sup> Bok<sup>+/+</sup> Tp53<sup>fl/fl</sup>* and the experiment was conducted as described for the previous cohorts. After 13 weeks of tumor development, mice were sacrificed and analysis with H&E staining, tumor burden analysis, and IHC staining was performed as in the prior experiments. As expected, I found that mice of all three genotypes had multiple fully developed adenocarcinomas. Interestingly, the difference in overall tumor burden between *Bok<sup>+/+</sup>* and *Bok<sup>-/-</sup>* that was present at 19 weeks in double transgenic mice was not seen in the p53-null lungs (Fig. 19A and D). Fittingly, the number and size of lesions were similar in this experiment regardless of BOK status (Fig. 19 B and C). The proliferative rates, appropriately, were similar in BOK-deficient and -proficient mice (Fig. 19E), as were the levels of DNA damage and p21 (Fig. 19F and G). The complete loss of phenotypic differences between the genotypes strongly indicates that BOK can only exert its role in the presence of the p53 protein or is somehow dependent on interaction with an intact p53 pathway.

Lastly, to confirm that this change in phenotype is not due to an increased immunologic response in response to a more aggressively growing tumor type, I analyzed six lesions per animal for CD3, CD45R, and F4/80. The levels of T- and B lymphocytes were similar in all genotypes (Fig. 20 A and B). The number of macrophages was statistically lower in BOK-deficient lesions, however this effect was driven by a single wildtype animal (Fig. 20C). Overall, it remains unlikely that the immune system plays an influential role in this setting.

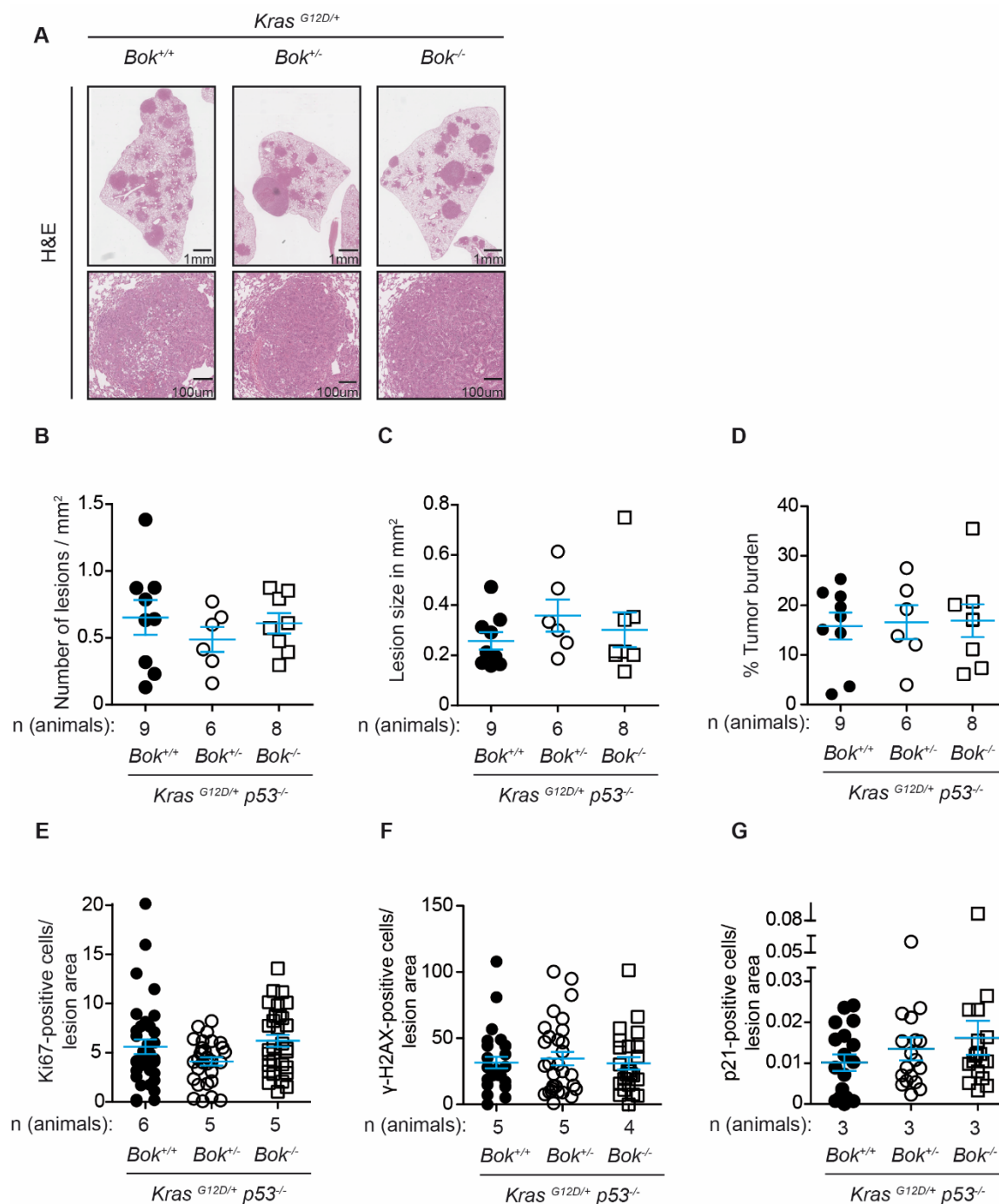


**Figure 19. Co-deletion of p53 eliminates the BOK-dependent phenotype.** (A) Representative images of H&E staining of lungs of the indicated genotypes 29 weeks after infection with AdenoCre. Bottom panels are higher magnification. (B) Number of lesions per total lung area in mm<sup>2</sup>, three slides averaged per animal. (C) Average lesion size in mm<sup>2</sup>, three slides averaged per animal. (D) Tumor burden calculated as tumor area (in mm<sup>2</sup>) divided by lung area (in mm<sup>2</sup>), three slides averaged per animal. Data analyzed by unpaired two-tailed t test and one-way ANOVA with post-hoc correction. Quantification of Ki67 staining (E), γ-H2AX staining (F), and p21 staining (G). Six lesions per animal were analyzed and presented as mean +/- SEM. Data are reported as number of positive cells

normalized to lesion area and analyzed by Kruskal-Wallis test with p-values from post hoc analysis. In part adapted from Meinhardt et al., 2022.

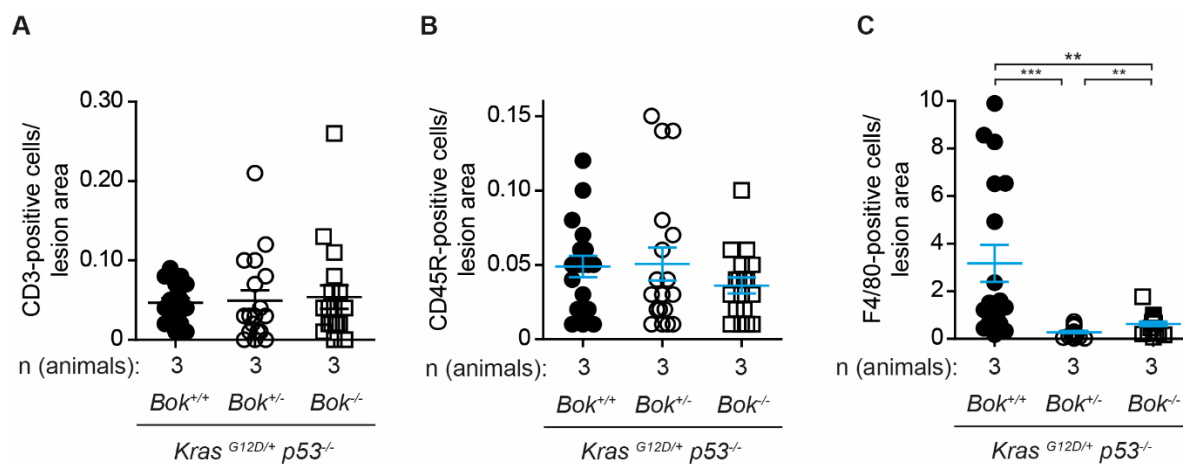


**Figure 20. Similar immune responses in triple transgenic mice.** Quantification of CD3 staining for T-lymphocytes, CD45R for B-lymphocytes and F4/80 for macrophages. Six lesions per animal were analyzed and presented as mean  $\pm$  SEM. Data are reported as number of positive cells normalized to lesion area and analyzed by Kruskal-Wallis test with p-values from post hoc analysis. (\*\*:  $p < 0.01$ , \*\*\*:  $p < 0.001$ )

## 4. Discussion

---

Lung cancer remains one of the most commonly diagnosed cancers and is the leading cause of cancer deaths worldwide (Global Cancer Observatory: Cancer Today. International Agency for Research on Cancer, 2024; Siegel et al., 2022). The implementation of public health measures and increased awareness of the toxicity of tobacco and other carcinogens have led to a slow decrease in lung cancer incidence in countries like the United States (Bade & Dela Cruz, 2020) (Thai et al., 2021). However, incidence is still rising in low-or-middle-income countries (Bade & Dela Cruz, 2020; Thai et al., 2021). Another significant portion of cases (10-20% in the U.S., for example) are not tobacco-related and therefore even harder to predict and diagnose in early stages (Shiels et al., 2024). Recently, screening of at-risk patients using low dose computed tomography has been established in some countries (Wolf et al., 2024), which is especially important due to the lack of clear symptoms in most patients. Many cases are diagnosed at later stages, often resulting in decreased survival rates (Bade & Dela Cruz, 2020). Despite the marked progress in understanding and targeting this disease that has been made in recent years, there remains a continued need for research in this field.

In 2000, Hanahan and Weinberg published a landmark paper on what they believed were the most important cellular mechanisms of tumorigenesis in all cancer types. These included, among others, self-sufficiency in growth signals, sustained angiogenesis, and evading apoptosis. These mechanisms were termed the hallmarks of cancer and have remained important pillars in our understanding of cancer (Hanahan & Weinberg, 2000). These hallmarks were even expanded upon in 2011, termed “The Next Generation”, as our understanding continues to evolve (Hanahan & Weinberg, 2011). Studying and finding ways to target these different mechanisms is crucial in the fight towards defeating cancer. The process of apoptosis is one of the original hallmarks and has remained an important concept since then. Since it is prominently governed by the BCL-2 family of proteins, it is reasonable to postulate that understanding these proteins and their interactions is paramount to elucidating and then weaponizing cell death in cancerous cells. The namesake protein BCL-2 was the first family member to be implicated in carcinogenesis, specifically in B-cell lymphomas (Warren, Wong-Brown, & Bowden, 2019). Since then, multiple other family members have been shown to play a role in cancer biology, as well as in therapeutic response.

With Beroukhim et al.'s discovery of *BOK* deletions in human cancer cells, this newer and less well understood BCL-2 family member was moved into the spotlight (Beroukhim et al., 2010). Could this protein be a key towards restoring or initiating apoptosis in cancer cells? Could it be a novel tumor suppressor? Consequently, we decided to further investigate the BCL-2-related ovarian killer in the context of lung adenocarcinoma.

The key finding in our work is that, contrary to initial assumptions, BOK is not simply a tumor suppressor in a BAX/BAK-like fashion. In our murine model of *Kras*<sup>G12D</sup>-driven lung adenocarcinoma, we found it to be the opposite – its presence seems to have a tumor promoting role during tumorigenesis. The absence of BOK in lesions after 19 weeks of tumor development led to a lower overall tumor burden in mice, which was driven by a lower number of lesions in these animals. Moreover, these lesions tended to be less aggressive in their histological phenotype compared to the wildtype controls. While this is contrary to some early studies, recent publications do point towards cell death-independent functions of BOK, including a pro-proliferative role of BOK, first proposed by Ray et al. (Ray et al., 2010). This is also in line with what Rabachini et al. found in their model of hepatocellular carcinoma (Rabachini et al., 2018). They were able to demonstrate that in diethylnitrosamine (DEN)-induced murine hepatocarcinogenesis, BOK-deficient animals had fewer and smaller lesions than the WT animals. Our immunohistochemical evaluation similarly revealed a decreased proliferative rate in the absence of BOK. This was supported by in vitro data, where *Bok*<sup>-/-</sup> murine lung cancer cells were shown to proliferate less and had a longer duration of cell cycle phase G2. Again, this was mirrored by Rabachini et al., who showed decreased proliferation in BOK-deficient HCC cell lines. Even more relevant to our data in lung tissue, is Zhang et al.'s finding that BOK overexpression in human bronchial epithelial (HBE) cells induced cellular proliferation in vitro (Zhang et al., 2019). Similarly, others found that, instead of being a pro-death effector, the absence of BOK in neurons increased their sensitivity to injury and death induced by oxygen deprivation, glucose deprivation, or staurosporine (D'Orsi et al., 2016).

In additional evaluations of our murine lung cancer lesions we found that BOK-deficiency lead to higher levels of DNA damage at 19 weeks compared to BOK-proficient animals, when evaluated by IHC. This was confirmed in vitro with a comet assay, where *Bok*<sup>-/-</sup> cells were more susceptible to developing DNA damage upon challenge with cytotoxic agents. In line with these findings, our *Bok*<sup>-/-</sup> cells were more susceptible to death from DNA damage-inducing agents, but not to agents

that act through other mechanisms. This is further supported by Zhang et al.'s finding that lower expression of BOK in healthy human bronchial epithelial cell lines lead to more extensive DNA damage in response to H<sub>2</sub>O<sub>2</sub> and cadmium chloride (Zhang et al., 2019). It is unclear at this time whether this propensity to damage could be one factor contributing to the lower tumor burden, through triggering cell senescence or death, or whether it promoted the tumor growth seen in 29-week mice through enabling accumulation of additional oncogenic mutations. Some have postulated that DNA damage leading to cell death can promote tumor development by causing enhanced proliferation of progenitor cells, which in turn sustains oncogenic genetic alterations (Rabachini et al., 2018).

To further understand the mechanisms through which BOK exerts its effects, we utilized co-deletion of p53 in our experimental setting. We were able to show that the absence of p53 during tumorigenesis in our lung lesions eliminated the phenotypic differences we had seen at 19 weeks. Instead, we found similar tumor burden, proliferative index, and DNA damage levels in all three genotypes. Our initial phenotype is therefore likely dependent on the presence of p53. Similarly, in our model of prolonged tumorigenesis to 29 weeks, we were unable to detect the phenotypic differences seen at the earlier timepoint. This could have various reasons, for example could the acquisition of additional oncogenic mutations during further progression of lesions outweigh the loss of BOK and render us unable to detect any differences based solely upon *Bok*-deletion. One such mutation could even be the loss of p53, which is known to occur in almost half of all human adenocarcinomas. Given the increased levels of DNA damage in *Bok*<sup>-/-</sup> animals after 19 weeks (and without simultaneously increased levels of apoptosis), it could be extrapolated that this may lead to a higher tumor mutational burden (TMB) and therefore be one factor leading to the accelerated tumor growth of *Bok*<sup>-/-</sup> lesions by 29 weeks. Interestingly, one publication looking at a mixture of squamous and adenocarcinoma samples found that BOK may specifically exert a tumor-suppressor-like function at later stages of disease (Moravcikova et al., 2017). In their experiments they found that BOK expression was significantly lower in less differentiated tumors (grades 2 and 3) as well as in lymph node-positive patients, while BOK levels were similar to healthy tissue in grade 1 lesions and node-negative patients. This could mean that in later stages, BOK-deficiency could promote tumor progression, while it leads to decreased growth earlier on. This highlights how valuable the information gained through our mouse model is, since we are

able to capture early stages of cancer development that are not usually seen in humans, and therefore supplement the information gathered from studies using patient samples.

Along these same lines of inquiry, Srivastava et al. found p53 to be induced in BOK-deficient cells (Srivastava et al., 2019). More specifically, they proposed that BOK may be a regulator of p53 levels (and therefore of proliferation) through impacting the nucleotide metabolism, since nucleotide deficiency is a recognized inducer of genome instability and p53 response (Srivastava et al., 2019). These results are in line with our findings, where in the absence of p53 any BOK-driven differences in our murine cancer model disappeared. It could be questioned whether, in our mouse models, the differences are driven by a ceiling effect due to the different aggressiveness of the tumor models. However, while this could explain the tumor burden, it could not justify the effects on proliferation and DNA damage.

Our hypothesis is further supported by our experiments evaluating lesions for p21 via IHC, as an important component of the p53 pathway. In this pathway, p21 has long been described as a regulator of DNA replication by facilitating DNA damage repair prior to replication when damage is present, for example through blocking CDK2 activity (Kulaberoglu, 2021). Fittingly, we found that levels of p21 were decreased in BOK-deficient lesions at the early timepoint, again indicating that lack of interaction with this p53 pathway may be responsible for the increased DNA damage. At the later timepoint however, p21 levels were slightly increased in *Bok*<sup>-/-</sup> lesions. Intriguingly, gene expression profiling of human HCT-116 colorectal carcinoma cells by Rabachini et al. demonstrated upregulation of genes related to cell cycle arrest and DNA damage response in BOK-deficient cells (Rabachini et al., 2018). Specifically, the proliferative defect described after downregulation of BOK was associated with higher levels of the cyclin kinase inhibitors p19<sup>INK4</sup> and p21<sup>cip1</sup> (Rabachini et al., 2018). More recently, p21 has been called a “dual effector”, as its function can also be oncogenic through promoting cell cycle progression or inhibiting apoptosis based on its cellular context, subcellular localization, and posttranscriptional modification (Kulaberoglu, 2021). The full extent of a potential BOK-p21-interaction therefore remains to be seen.

Some have proposed that apoptosis induction and proliferation inhibition are largely the same process. It is known that apoptosis and cellular proliferation are linked by cell-cycle regulators and signaling pathways that affect both processes (Alenzi, 2004). Under physiologic conditions,



Taken together, our data clearly show that presence of the BOK protein promotes proliferation of tumor cells in mutant *Kras*-driven lung cancer, especially in early tumorigenesis, and is vital in cellular response to DNA damage. Therefore, this BCL-2 family member, which to date remains poorly understood, warrants continued examination to fully elucidate its function and potentially harvest this knowledge for clinical benefit.

## 5. Outlook

---

While our work sheds further light on the role of BOK in general, and more specifically its place in lung adenocarcinoma, there is more work that needs to be done. We evaluated this gene of interest in a whole-body knockout system, as this is a reliable way to obtain loss of BOK in all cancer cells, and in order to make generalizable conclusions of cancer cell processes. However, the downside of this is the concurrent BOK-deficiency of other cells involved in tumorigenesis, such as the immune system. While previous studies of whole-body BOK-deficient animals did not reveal any essential differences at steady state, this has not been specifically evaluated in lung cancer in vivo and could theoretically have a yet-to-be-characterized impact.

Both pro- and anti-apoptotic roles, as well as non-apoptosis-related functions, have been suggested by the various groups investigating BOK. These include associations with ER stress, DNA damage and uridine metabolism, to name a few. Which of these roles are crucial in its role in tumorigenesis remains to be seen. Based on our data, an association with DNA damage, the p53 pathway, and subsequent impact on cellular proliferation seen to be key. It is possible, however, that its function may be tissue dependent. Different cancer types with their specific cells of origin, metabolic requirements, driver mutations, microenvironments or metastatic behaviors may depend on BOK in wholly different ways.

Targeting of other BCL-2 family members has become possible in recent years, such as with the BCL-2 inhibitor ABT-199 (Venetoclax). Development of a BOK inhibitor, to utilize in vivo in murine models of cancer during different stages of cancer development could shed light on its role in tumors, especially over time. Alternatively, targeted in vivo knockdown, in a fashion similar to our AdenoCre instillation model, could be utilized to this end. Is BOK-deficiency most impactful early in tumorigenesis? Or rather later on? Or could its function change and evolve together with the cancer cell? Furthermore, given the controversial in vitro data of whether BOK overexpression truly induces apoptosis, the approach of restoring or amplifying BOK in mice, e.g. through AdenoCre or CRISPR-Cas9-mediated genome editing, could also prove insightful.

Given the differential response of cell lines to DNA damage inducing agents, another approach could be treatment of animals with established lung cancer and evaluating their different treatment

responses. Could the level of BOK expression be utilized in patients to target their chemotherapy regimen and predict therapeutic response?

In summary, while there is still much to be understood about this BCL-2 family member, the available data points to an important function of BOK that remains important to study going forward.

## 6. Abbreviations

---

4-OHT	4-hydroxytamoxifen
5-FU	5-fluorouracil
AAH	Atypical adenomatous hyperplasia
AB-PAS	Alcian Blue and Periodic Acid Schiff staining
ALK	Anaplastic lymphoma kinase
ATP	Adenosine triphosphate
BAD	BCL-2-associated agonist of cell death
BAK	BCL-2 antagonist/killer
BAX	BCL-2-associated X-protein
BCA assay	Bicinchoninic assay
BCL-xL	B-cell lymphoma extra large
BCL-2	B-cell lymphoma-2
BIK	BCL-2-interacting killer
BIM	BCL-2-interacting mediator of cell death
BOK	BCL-2 related ovarian killer
BRAF	v-RAF murine sarcoma viral oncogene homolog B1
CC10	Clara cell antigen 10
CD	Cluster of differentiation
CDK2	Cyclin-dependent kinase
CK5/6	Cytokeratin 5/6
cm	Centimeter
CO <sub>2</sub>	Carbon dioxide
CRISPR	Clustered Regularly Interspaced Short Palindromic Repeats
ctDNA	Circulating tumor DNA
DAB	3,3-diaminobenzidine
DEN	Diethylnitrosamine
DMEM	Dulbecco's Modified Eagle Medium
DNA	Deoxyribonucleic acid
EDTA	Ethylenediaminetetraacetic acid

EGFR	Epidermal growth factor receptor
EML4-ALK	Echinoderm microtubule-associated protein-like 4-anaplastic lymphoma kinase
ER	Endoplasmic reticulum
FBS	Fetal bovine serum
FCCP	Carbonyl cyanide-4 (trifluoromethoxy) phenylhydrazone
FDG	Fluorodeoxyglucose
FFPE	Formalin fixed paraffin embedded
GEMM	Genetically engineered mouse model
GFP	Green fluorescent protein
GTP	Guanosine triphosphate
h	Hour
H&E	Hematoxylin and eosin
HBE	Human bronchial epithelium
HCC	Hepatocellular carcinoma
I <sub>2</sub> E	1% iodine (I <sub>2</sub> ) dissolved in absolute ethanol
IHC	Immunohistochemistry
IP <sub>3</sub>	1,4,5-trisphosphate receptors
kDa	Kilodalton
kg	Kilogram
KRAS	Kirsten rat sarcoma viral oncogene homolog
LDCT	Low-dose computed tomography
LUAD	Lung adenocarcinoma
LUSC	Lung squamous cell carcinoma
MAPK	Mitogen-activated protein kinase
MCA	3-methylcholanthrene
MCL-1	Myeloid cell leukemia-1
MEF	Murine embryonic fibroblast
MEK	Mitogen-activated protein kinase
MET	Mesenchymal epithelial transcription factor
μg	Microgram
mg	Milligram
min	Minute
ml	Milliliter

$\mu\text{M}$	Micromole
mM	Millimole
MMF	Medetomidine, midazolam, fentanyl
MOMP	Mitochondrial outer membrane permeabilization
MRI	Magnetic resonance imaging
NSCLC	Non-small cell lung cancer
NTCU	N-nitroso-tris-chloroethyl urea
PCR	Polymerase chain reaction
PD-1	Programmed death-1
PD-L1	Programmed death-ligand 1
PET	Positron emission tomography
PFU	Plaque-forming unit
PI3K	Phosphatidylinositol-3-kinase
RAF	Rapidly accelerated fibrosarcoma
RAS	Rat sarcoma viral oncogene homolog
RNA	Ribonucleic acid
RPMI	Roswell Park Memorial Institute
SCC	Squamous cell carcinoma
SCLC	Small cell lung cancer
SDS-PAGE	Sodium dodecyl sulfate polyacrylamide gel electrophoresis
SP-C	Surfactant protein-C
TCGA	The cancer genome atlas
TMB	Tumor mutational burden
TTF-1	Thyroid transcription factor-1
UMP	Uridine monophosphate
WHO	World health organization
WT	Wildtype

## 7. Acknowledgements

---

*If I have seen further, it is by standing on the shoulders of giants.*

Isaac Newton

First, I want to thank Prof. Dr. Philipp Jost for allowing me to become part of his team and work on this project, for his guidance, his encouragement, and for taking a chance on a student who barely knew how to hold a pipette.

I would also like to thank my fellow members of the AG Jost, without whom none of this work would have been possible. I am incredibly thankful to Dr. Enkhtsetseg Munkhbaatar, who taught me all about mice and lung cancer, and who remained my mentor and inspiration throughout. Additionally, Ulrike Höckendorf was always available to help, brainstorm, and discuss the many mysteries of BOK. And thank you to Caterina Branca, for helping in the final touches of the project and published manuscript, and to Xin Wang for teaching me about TCGA. I also could not have performed any experiments without the initial training by Stephanie Rott.

To the other members of AG Jost, I am thankful for creating a supportive working environment and for making science a joyous experience.

I thank Dr. Martina Anton for her collaboration and input in facilitating the adenoviral infections.

For their knowledge and assistance regarding all things histology and immunohistochemistry, I would also like to express my gratitude to Dr. Katja Steiger and Anne Jacob.

Special thanks also goes to Prof. Dr. Julia Herzen, Pidassa Bidola, and Kirsten Taphorn for their knowhow and collaboration on imaging.

I would also like to acknowledge our neighbors AG Ruland, whose resources and expertise helped me accomplish many of these experiments.

Lastly, but most certainly not least, I would like to thank my family. To my parents I am thankful for always believing in me, even when I didn't. For making me set higher standards, for being supportive, for occasionally giving me the proverbial "kick in the behind", and for being proud of me when I couldn't always find a reason to be. My aunts, grandparents, and brother. My safety net. This is for you.

## 8. References

---

### Own publications:

- Bidola, P., Martins de Souza, E. S. J., Achterhold, K., Munkhbaatar, E., Jost, P. J., **Meinhardt, A. L.**, Taphorn, K., Zdora, M. C., Pfeiffer, F., & Herzen, J. (2019). A step towards valid detection and quantification of lung cancer volume in experimental mice with contrast agent-based X-ray microtomography. *Sci Rep*, *9*(1), 1325. <https://doi.org/10.1038/s41598-018-37394-w>
- Meinhardt, A. L.**, Munkhbaatar, E., Höckendorf, U., Dietzen, M., Dechant, M., Anton, M., Jacob, A., Steiger, K., Weichert, W., Brcic, L., McGranahan, N., Branca, C., Kaufmann, T., Dengler, M. A., & Jost, P. J. (2022). The BCL-2 family member BOK promotes KRAS-driven lung cancer progression in a p53-dependent manner. *Oncogene*, *41*(9), 1376-1382. <https://doi.org/10.1038/s41388-021-02161-1>
- Munkhbaatar, E., Dietzen, M., Agrawal, D., Anton, M., Jesinghaus, M., Boxberg, M., Pfarr, N., Bidola, P., Uhrig, S., Höckendorf, U., **Meinhardt, A. L.**, Wahida, A., Heid, I., Braren, R., Mishra, R., Warth, A., Muley, T., Poh, P. S. P., Wang, X., . . . Jost, P. J. (2020). MCL-1 gains occur with high frequency in lung adenocarcinoma and can be targeted therapeutically. *Nat Commun*, *11*(1), 4527. <https://doi.org/10.1038/s41467-020-18372-1>

### General references:

- Alavian, K. N., Li, H., Collis, L., Bonanni, L., Zeng, L., Sacchetti, S., Lazrove, E., Nabili, P., Flaherty, B., Graham, M., Chen, Y., Messerli, S. M., Mariggio, M. A., Rahner, C., McNay, E., Shore, G. C., Smith, P. J., Hardwick, J. M., & Jonas, E. A. (2011). Bcl-xL regulates metabolic efficiency of neurons through interaction with the mitochondrial F1FO ATP synthase. *Nat Cell Biol*, *13*(10), 1224-1233. <https://doi.org/10.1038/ncb2330>
- Alenzi, F. Q. (2004). Links between apoptosis, proliferation and the cell cycle. *Br J Biomed Sci*, *61*(2), 99-102. <https://doi.org/10.1080/09674845.2004.11732652>
- Bade, B. C., & Dela Cruz, C. S. (2020). Lung Cancer 2020: Epidemiology, Etiology, and Prevention. *Clin Chest Med*, *41*(1), 1-24. <https://doi.org/10.1016/j.ccm.2019.10.001>
- Beroukhim, R., Mermel, C. H., Porter, D., Wei, G., Raychaudhuri, S., Donovan, J., Barretina, J., Boehm, J. S., Dobson, J., Urashima, M., Mc Henry, K. T., Pinchback, R. M., Ligon, A. H., Cho, Y. J., Haery, L., Greulich, H., Reich, M., Winckler, W., Lawrence, M. S., . . . Meyerson, M. (2010). The landscape of somatic copy-number alteration across human cancers. *Nature*, *463*(7283), 899-905. <https://doi.org/10.1038/nature08822>

- Bidola, P., Martins de Souza, E. S. J., Achterhold, K., Munkhbaatar, E., Jost, P. J., Meinhardt, A. L., Taphorn, K., Zdora, M. C., Pfeiffer, F., & Herzen, J. (2019). A step towards valid detection and quantification of lung cancer volume in experimental mice with contrast agent-based X-ray microtomography. *Sci Rep*, *9*(1), 1325. <https://doi.org/10.1038/s41598-018-37394-w>
- Bonzerato, C. G., & Wojcikiewicz, R. J. H. (2023). Bok: real killer or bystander with non-apoptotic roles? *Front Cell Dev Biol*, *11*, 1161910. <https://doi.org/10.3389/fcell.2023.1161910>
- Brock, C. K., Wallin, S. T., Ruiz, O. E., Samms, K. M., Mandal, A., Sumner, E. A., & Eisenhoffer, G. T. (2019). Stem cell proliferation is induced by apoptotic bodies from dying cells during epithelial tissue maintenance. *Nat Commun*, *10*(1), 1044. <https://doi.org/10.1038/s41467-019-09010-6>
- Campbell, K. J., & Tait, S. W. G. (2018). Targeting BCL-2 regulated apoptosis in cancer. *Open Biol*, *8*(5). <https://doi.org/10.1098/rsob.180002>
- Carpio, M. A., Michaud, M., Zhou, W., Fisher, J. K., Walensky, L. D., & Katz, S. G. (2015). BCL-2 family member BOK promotes apoptosis in response to endoplasmic reticulum stress. *Proc Natl Acad Sci U S A*, *112*(23), 7201-7206. <https://doi.org/10.1073/pnas.1421063112>
- Chevallier, M., Borgeaud, M., Addeo, A., & Friedlaender, A. (2021). Oncogenic driver mutations in non-small cell lung cancer: Past, present and future. *World J Clin Oncol*, *12*(4), 217-237. <https://doi.org/10.5306/wjco.v12.i4.217>
- Cory, S., Huang, D. C., & Adams, J. M. (2003). The Bcl-2 family: roles in cell survival and oncogenesis. *Oncogene*, *22*(53), 8590-8607. <https://doi.org/10.1038/sj.onc.1207102>
- D'Orsi, B., Engel, T., Pfeiffer, S., Nandi, S., Kaufmann, T., Henshall, D. C., & Prehn, J. H. (2016). Bok Is Not Pro-Apoptotic But Suppresses Poly ADP-Ribose Polymerase-Dependent Cell Death Pathways and Protects against Excitotoxic and Seizure-Induced Neuronal Injury. *J Neurosci*, *36*(16), 4564-4578. <https://doi.org/10.1523/jneurosci.3780-15.2016>
- Danial, N. N., Gramm, C. F., Scorrano, L., Zhang, C. Y., Krauss, S., Ranger, A. M., Datta, S. R., Greenberg, M. E., Licklider, L. J., Lowell, B. B., Gygi, S. P., & Korsmeyer, S. J. (2003). BAD and glucokinase reside in a mitochondrial complex that integrates glycolysis and apoptosis. *Nature*, *424*(6951), 952-956. <https://doi.org/10.1038/nature01825>
- Danial, N. N., Walensky, L. D., Zhang, C. Y., Choi, C. S., Fisher, J. K., Molina, A. J., Datta, S. R., Pitter, K. L., Bird, G. H., Wikstrom, J. D., Deeney, J. T., Robertson, K., Morash, J., Kulkarni, A., Neschen, S., Kim, S., Greenberg, M. E., Corkey, B. E., Shirihai, O. S., . . . Korsmeyer, S. J. (2008). Dual role of proapoptotic BAD in insulin secretion and beta cell survival. *Nat Med*, *14*(2), 144-153. <https://doi.org/10.1038/nm1717>
- Donehower, L. A., Soussi, T., Korkut, A., Liu, Y., Schultz, A., Cardenas, M., Li, X., Babur, O., Hsu, T. K., Lichtarge, O., Weinstein, J. N., Akbani, R., & Wheeler, D. A. (2019). Integrated Analysis of TP53 Gene and Pathway Alterations in The Cancer Genome Atlas. *Cell Rep*, *28*(5), 1370-1384.e1375. <https://doi.org/10.1016/j.celrep.2019.07.001>

- Duma, N., Santana-Davila, R., & Molina, J. R. (2019). Non-Small Cell Lung Cancer: Epidemiology, Screening, Diagnosis, and Treatment. *Mayo Clin Proc*, *94*(8), 1623-1640. <https://doi.org/10.1016/j.mayocp.2019.01.013>
- Echeverry, N., Bachmann, D., Ke, F., Strasser, A., Simon, H. U., & Kaufmann, T. (2013). Intracellular localization of the BCL-2 family member BOK and functional implications. *Cell Death Differ*, *20*(6), 785-799. <https://doi.org/10.1038/cdd.2013.10>
- Engelman, J. A., Chen, L., Tan, X., Crosby, K., Guimaraes, A. R., Upadhyay, R., Maira, M., McNamara, K., Perera, S. A., Song, Y., Chirieac, L. R., Kaur, R., Lightbown, A., Simendinger, J., Li, T., Padera, R. F., García-Echeverría, C., Weissleder, R., Mahmood, U., . . . Wong, K. K. (2008). Effective use of PI3K and MEK inhibitors to treat mutant Kras G12D and PIK3CA H1047R murine lung cancers. *Nat Med*, *14*(12), 1351-1356. <https://doi.org/10.1038/nm.1890>
- Fannjiang, Y., Kim, C. H., Haganir, R. L., Zou, S., Lindsten, T., Thompson, C. B., Mito, T., Traystman, R. J., Larsen, T., Griffin, D. E., Mandir, A. S., Dawson, T. M., Dike, S., Sappington, A. L., Kerr, D. A., Jonas, E. A., Kaczmarek, L. K., & Hardwick, J. M. (2003). BAK alters neuronal excitability and can switch from anti- to pro-death function during postnatal development. *Dev Cell*, *4*(4), 575-585. [https://doi.org/10.1016/s1534-5807\(03\)00091-1](https://doi.org/10.1016/s1534-5807(03)00091-1)
- Fernandez-Marrero, Y., Ke, F., Echeverry, N., Bouillet, P., Bachmann, D., Strasser, A., & Kaufmann, T. (2016). Is BOK required for apoptosis induced by endoplasmic reticulum stress? *Proc Natl Acad Sci U S A*, *113*(5), E492-493. <https://doi.org/10.1073/pnas.1516347113>
- Fisher, G. H., Wellen, S. L., Klimstra, D., Lenczowski, J. M., Tichelaar, J. W., Lizak, M. J., Whitsett, J. A., Koretsky, A., & Varmus, H. E. (2001). Induction and apoptotic regression of lung adenocarcinomas by regulation of a K-Ras transgene in the presence and absence of tumor suppressor genes. *Genes Dev*, *15*(24), 3249-3262. <https://doi.org/10.1101/gad.947701>
- Global Cancer Observatory: Cancer Today. International Agency for Research on Cancer. (2024). : International Agency for Research on Cancer. Retrieved April 2024 from <https://gco.iarc.who.int/en>
- Gross, A., & Katz, S. G. (2017). Non-apoptotic functions of BCL-2 family proteins. *Cell Death Differ*, *24*(8), 1348-1358. <https://doi.org/10.1038/cdd.2017.22>
- Guerra, C., Mijimolle, N., Dhawahir, A., Dubus, P., Barradas, M., Serrano, M., Campuzano, V., & Barbacid, M. (2003). Tumor induction by an endogenous K-ras oncogene is highly dependent on cellular context. *Cancer Cell*, *4*(2), 111-120. [https://doi.org/10.1016/s1535-6108\(03\)00191-0](https://doi.org/10.1016/s1535-6108(03)00191-0)
- Han, Y., Liu, D., & Li, L. (2020). PD-1/PD-L1 pathway: current researches in cancer. *Am J Cancer Res*, *10*(3), 727-742.
- Hanahan, D., & Weinberg, R. A. (2000). The hallmarks of cancer. *Cell*, *100*(1), 57-70. [https://doi.org/10.1016/s0092-8674\(00\)81683-9](https://doi.org/10.1016/s0092-8674(00)81683-9)
- Hanahan, D., & Weinberg, R. A. (2011). Hallmarks of cancer: the next generation. *Cell*, *144*(5), 646-674. <https://doi.org/10.1016/j.cell.2011.02.013>

- Hsu, S. Y., Kaipia, A., McGee, E., Lomeli, M., & Hsueh, A. J. (1997). Bok is a pro-apoptotic Bcl-2 protein with restricted expression in reproductive tissues and heterodimerizes with selective anti-apoptotic Bcl-2 family members. *Proc Natl Acad Sci U S A*, *94*(23), 12401-12406. <https://doi.org/10.1073/pnas.94.23.12401>
- Hu, J., Cao, J., Topatana, W., Juengpanich, S., Li, S., Zhang, B., Shen, J., Cai, L., Cai, X., & Chen, M. (2021). Targeting mutant p53 for cancer therapy: direct and indirect strategies. *J Hematol Oncol*, *14*(1), 157. <https://doi.org/10.1186/s13045-021-01169-0>
- Hynds, R. E., Frese, K. K., Pearce, D. R., Grönroos, E., Dive, C., & Swanton, C. (2021). Progress towards non-small-cell lung cancer models that represent clinical evolutionary trajectories. *Open Biol*, *11*(1), 200247. <https://doi.org/10.1098/rsob.200247>
- Inamura, K. (2018). Update on Immunohistochemistry for the Diagnosis of Lung Cancer. *Cancers (Basel)*, *10*(3). <https://doi.org/10.3390/cancers10030072>
- Ionescu, D. N., Stockley, T. L., Banerji, S., Couture, C., Mather, C. A., Xu, Z., Blais, N., Cheema, P. K., Chu, Q. S., Melosky, B., & Leighl, N. B. (2022). Consensus Recommendations to Optimize Testing for New Targetable Alterations in Non-Small Cell Lung Cancer. *Curr Oncol*, *29*(7), 4981-4997. <https://doi.org/10.3390/curroncol29070396>
- Islami, F., Goding Sauer, A., Miller, K. D., Siegel, R. L., Fedewa, S. A., Jacobs, E. J., McCullough, M. L., Patel, A. V., Ma, J., Soerjomataram, I., Flanders, W. D., Brawley, O. W., Gapstur, S. M., & Jemal, A. (2018). Proportion and number of cancer cases and deaths attributable to potentially modifiable risk factors in the United States. *CA Cancer J Clin*, *68*(1), 31-54. <https://doi.org/10.3322/caac.21440>
- Iwanaga, K., Yang, Y., Raso, M. G., Ma, L., Hanna, A. E., Thilaganathan, N., Moghaddam, S., Evans, C. M., Li, H., Cai, W. W., Sato, M., Minna, J. D., Wu, H., Creighton, C. J., Demayo, F. J., Wistuba, II, & Kurie, J. M. (2008). Pten inactivation accelerates oncogenic K-ras-initiated tumorigenesis in a mouse model of lung cancer. *Cancer Res*, *68*(4), 1119-1127. <https://doi.org/10.1158/0008-5472.Can-07-3117>
- Jackson, E. L., Olive, K. P., Tuveson, D. A., Bronson, R., Crowley, D., Brown, M., & Jacks, T. (2005). The differential effects of mutant p53 alleles on advanced murine lung cancer. *Cancer Res*, *65*(22), 10280-10288. <https://doi.org/10.1158/0008-5472.Can-05-2193>
- Jackson, E. L., Willis, N., Mercer, K., Bronson, R. T., Crowley, D., Montoya, R., Jacks, T., & Tuveson, D. A. (2001). Analysis of lung tumor initiation and progression using conditional expression of oncogenic K-ras. *Genes Dev*, *15*(24), 3243-3248. <https://doi.org/10.1101/gad.943001>
- Ji, H., Ramsey, M. R., Hayes, D. N., Fan, C., McNamara, K., Kozlowski, P., Torrice, C., Wu, M. C., Shimamura, T., Perera, S. A., Liang, M. C., Cai, D., Naumov, G. N., Bao, L., Contreras, C. M., Li, D., Chen, L., Krishnamurthy, J., Koivunen, J., . . . Wong, K. K. (2007). LKB1 modulates lung cancer differentiation and metastasis. *Nature*, *448*(7155), 807-810. <https://doi.org/https://doi.org/10.1038/nature06030>
- Johnson, L., Mercer, K., Greenbaum, D., Bronson, R. T., Crowley, D., Tuveson, D. A., & Jacks, T. (2001). Somatic activation of the K-ras oncogene causes early onset lung cancer in mice. *Nature*, *410*(6832), 1111-1116. <https://doi.org/10.1038/35074129>

- Kale, J., Osterlund, E. J., & Andrews, D. W. (2018). BCL-2 family proteins: changing partners in the dance towards death. *Cell Death Differ*, *25*(1), 65-80. <https://doi.org/10.1038/cdd.2017.186>
- Ke, F., Bouillet, P., Kaufmann, T., Strasser, A., Kerr, J., & Voss, A. K. (2013). Consequences of the combined loss of BOK and BAK or BOK and BAX. *Cell Death Dis*, *4*(6), e650. <https://doi.org/10.1038/cddis.2013.176>
- Ke, F., Grabow, S., Kelly, G. L., Lin, A., O'Reilly, L. A., & Strasser, A. (2015). Impact of the combined loss of BOK, BAX and BAK on the hematopoietic system is slightly more severe than compound loss of BAX and BAK. *Cell Death Dis*, *6*(10), e1938. <https://doi.org/10.1038/cddis.2015.304>
- Ke, F., Voss, A., Kerr, J. B., O'Reilly, L. A., Tai, L., Echeverry, N., Bouillet, P., Strasser, A., & Kaufmann, T. (2012). BCL-2 family member BOK is widely expressed but its loss has only minimal impact in mice. *Cell Death Differ*, *19*(6), 915-925. <https://doi.org/10.1038/cdd.2011.210>
- Kulaberoglu, Y. H., A.; Gómez, V. (2021). The role of p53/p21/p16 in DNA damage signaling and DNA repair. In O. K. Igor Kovalchuk (Ed.), *Genome Stability (Second Edition)* (Vol. 26, pp. 257-274). Academic Press. <https://doi.org/https://doi.org/10.1016/B978-0-323-85679-9.00015-5>
- Kwon, M. C., & Berns, A. (2013). Mouse models for lung cancer. *Mol Oncol*, *7*(2), 165-177. <https://doi.org/10.1016/j.molonc.2013.02.010>
- Li, B., & Dewey, C. N. (2011). RSEM: accurate transcript quantification from RNA-Seq data with or without a reference genome. *BMC Bioinformatics*, *12*, 323. <https://doi.org/10.1186/1471-2105-12-323>
- Llambi, F., Wang, Y. M., Victor, B., Yang, M., Schneider, D. M., Gingras, S., Parsons, M. J., Zheng, J. H., Brown, S. A., Pelletier, S., Moldoveanu, T., Chen, T., & Green, D. R. (2016). BOK Is a Non-canonical BCL-2 Family Effector of Apoptosis Regulated by ER-Associated Degradation. *Cell*, *165*(2), 421-433. <https://doi.org/10.1016/j.cell.2016.02.026>
- Marino, S., Vooijs, M., van Der Gulden, H., Jonkers, J., & Berns, A. (2000). Induction of medulloblastomas in p53-null mutant mice by somatic inactivation of Rb in the external granular layer cells of the cerebellum. *Genes Dev*, *14*(8), 994-1004.
- Meinhardt, A. L., Munkhbaatar, E., Höckendorf, U., Dietzen, M., Dechant, M., Anton, M., Jacob, A., Steiger, K., Weichert, W., Brcic, L., McGranahan, N., Branca, C., Kaufmann, T., Dengler, M. A., & Jost, P. J. (2022). The BCL-2 family member BOK promotes KRAS-driven lung cancer progression in a p53-dependent manner. *Oncogene*, *41*(9), 1376-1382. <https://doi.org/10.1038/s41388-021-02161-1>
- Meuwissen, R., & Berns, A. (2005). Mouse models for human lung cancer. *Genes Dev*, *19*(6), 643-664. <https://doi.org/10.1101/gad.1284505>
- Meuwissen, R., Linn, S. C., van der Valk, M., Mooi, W. J., & Berns, A. (2001). Mouse model for lung tumorigenesis through Cre/lox controlled sporadic activation of the K-Ras oncogene. *Oncogene*, *20*(45), 6551-6558. <https://doi.org/10.1038/sj.onc.1204837>

- Moravcikova, E., Krepela, E., Donnenberg, V. S., Donnenberg, A. D., Benkova, K., Rabachini, T., Fernandez-Marrero, Y., Bachmann, D., & Kaufmann, T. (2017). BOK displays cell death-independent tumor suppressor activity in non-small-cell lung carcinoma. *Int J Cancer*, *141*(10), 2050-2061. <https://doi.org/10.1002/ijc.30906>
- Munkhbaatar, E., Dietzen, M., Agrawal, D., Anton, M., Jesinghaus, M., Boxberg, M., Pfarr, N., Bidola, P., Uhrig, S., Höckendorf, U., Meinhardt, A. L., Wahida, A., Heid, I., Braren, R., Mishra, R., Warth, A., Muley, T., Poh, P. S. P., Wang, X., . . . Jost, P. J. (2020). MCL-1 gains occur with high frequency in lung adenocarcinoma and can be targeted therapeutically. *Nat Commun*, *11*(1), 4527. <https://doi.org/10.1038/s41467-020-18372-1>
- Naim, S., & Kaufmann, T. (2020). The Multifaceted Roles of the BCL-2 Family Member BOK. *Front Cell Dev Biol*, *8*, 574338. <https://doi.org/10.3389/fcell.2020.574338>
- National Comprehensive Cancer Network. (2024). *NCCN Clinical Practice Guidelines in Oncology: Non-Small Cell Lung Cancer*. [https://www.nccn.org/professionals/physician\\_gls/pdf/nscl.pdf](https://www.nccn.org/professionals/physician_gls/pdf/nscl.pdf)
- Nettesheim, P., & Hammons, A. S. (1971). Induction of squamous cell carcinoma in the respiratory tract of mice. *J Natl Cancer Inst*, *47*(3), 697–701.
- Nikitin, A. Y., Alcaraz, A., Anver, M. R., Bronson, R. T., Cardiff, R. D., Dixon, D., Fraire, A. E., Gabrielson, E. W., Gunning, W. T., Haines, D. C., Kaufman, M. H., Linnoila, R. I., Maronpot, R. R., Rabson, A. S., Reddick, R. L., Rehm, S., Rozengurt, N., Schuller, H. M., Shmidt, E. N., . . . Jacks, T. (2004). Classification of proliferative pulmonary lesions of the mouse: recommendations of the mouse models of human cancers consortium. *Cancer Res*, *64*(7), 2307-2316. <https://doi.org/10.1158/0008-5472.can-03-3376>
- O'Leary, C., Gasper, H., Sahin, K. B., Tang, M., Kulasinghe, A., Adams, M. N., Richard, D. J., & O'Byrne, K. J. (2020). Epidermal Growth Factor Receptor (EGFR)-Mutated Non-Small-Cell Lung Cancer (NSCLC). *Pharmaceuticals (Basel)*, *13*(10). <https://doi.org/10.3390/ph13100273>
- Pawelczyk, K., Piotrowska, A., Ciesielska, U., Jablonska, K., Gletzel-Plucinska, N., Grzegorzolka, J., Podhorska-Okolow, M., Dziegiel, P., & Nowinska, K. (2019). Role of PD-L1 Expression in Non-Small Cell Lung Cancer and Their Prognostic Significance according to Clinicopathological Factors and Diagnostic Markers. *Int J Mol Sci*, *20*(4). <https://doi.org/10.3390/ijms20040824>
- Pelosi, G., Barbareschi, M., Cavazza, A., Graziano, P., Rossi, G., & Papotti, M. (2015). Large cell carcinoma of the lung: a tumor in search of an author. A clinically oriented critical reappraisal. *Lung Cancer*, *87*(3), 226-231. <https://doi.org/10.1016/j.lungcan.2015.01.008>
- Planchard, D., Popat, S., Kerr, K., Novello, S., Smit, E. F., Faivre-Finn, C., Mok, T. S., Reck, M., Van Schil, P. E., Hellmann, M. D., & Peters, S. (2018). Metastatic non-small cell lung cancer: ESMO Clinical Practice Guidelines for diagnosis, treatment and follow-up. *Ann Oncol*, *29*(Suppl 4), iv192-iv237. <https://doi.org/10.1093/annonc/mdy275>
- Politi, K., Zakowski, M. F., Fan, P. D., Schonfeld, E. A., Pao, W., & Varmus, H. E. (2006). Lung adenocarcinomas induced in mice by mutant EGF receptors found in human lung cancers respond to a tyrosine kinase inhibitor or to down-regulation of the receptors. *Genes Dev*, *20*(11), 1496-1510. <https://doi.org/10.1101/gad.1417406>

- Rabachini, T., Fernandez-Marrero, Y., Montani, M., Loforese, G., Sladky, V., He, Z., Bachmann, D., Wicki, S., Villunger, A., Stroka, D., & Kaufmann, T. (2018). BOK promotes chemical-induced hepatocarcinogenesis in mice. *Cell Death Differ*, 25(4), 708-720. <https://doi.org/10.1038/s41418-017-0008-0>
- Rampino, N., Yamamoto, H., Ionov, Y., Li, Y., Sawai, H., Reed, J. C., & Perucho, M. (1997). Somatic frameshift mutations in the BAX gene in colon cancers of the microsatellite mutator phenotype. *Science*, 275(5302), 967-969. <https://doi.org/10.1126/science.275.5302.967>
- Ray, J. E., Garcia, J., Jurisicova, A., & Caniggia, I. (2010). Mtd/Bok takes a swing: proapoptotic Mtd/Bok regulates trophoblast cell proliferation during human placental development and in preeclampsia. *Cell Death Differ*, 17(5), 846-859. <https://doi.org/10.1038/cdd.2009.167>
- Reck, M., Carbone, D. P., Garassino, M., & Barlesi, F. (2021). Targeting KRAS in non-small-cell lung cancer: recent progress and new approaches. *Ann Oncol*, 32(9), 1101-1110. <https://doi.org/10.1016/j.annonc.2021.06.001>
- Regales, L., Balak, M. N., Gong, Y., Politi, K., Sawai, A., Le, C., Koutcher, J. A., Solit, D. B., Rosen, N., Zakowski, M. F., & Pao, W. (2007). Development of new mouse lung tumor models expressing EGFR T790M mutants associated with clinical resistance to kinase inhibitors. *PLoS One*, 2(8), e810. <https://doi.org/https://doi.org/10.1371/journal.pone.0000810>
- Saffiotti, U., Cefis, F., & Kolb, L. H. (1968). A method for the experimental induction of bronchogenic carcinoma. *Cancer Res*, 28(1), 104-124.
- Scholzen, T., & Gerdes, J. (2000). The Ki-67 protein: from the known and the unknown. *J Cell Physiol*, 182(3), 311-322. [https://doi.org/10.1002/\(sici\)1097-4652\(200003\)182:3<311::Aid-jcp1>3.0.Co;2-9](https://doi.org/10.1002/(sici)1097-4652(200003)182:3<311::Aid-jcp1>3.0.Co;2-9)
- Schulman, J. J., Wright, F. A., Kaufmann, T., & Wojcikiewicz, R. J. H. (2013). The Bcl-2 protein family member Bok binds to the coupling domain of inositol 1,4,5-trisphosphate receptors and protects them from proteolytic cleavage. *J Biol Chem*, 288(35), 25340-25349. <https://doi.org/10.1074/jbc.M113.496570>
- Shiels, M. S., Graubard, B. I., McNeel, T. S., Kahle, L., & Freedman, N. D. (2024). Trends in smoking-attributable and smoking-unrelated lung cancer death rates in the United States, 1991-2018. *J Natl Cancer Inst*, 116(5), 711-716. <https://doi.org/10.1093/jnci/djad256>
- Shimkin, M. B., & Stoner, G. D. (1975). Lung tumors in mice: application to carcinogenesis bioassay. *Adv Cancer Res*, 21, 1-58. [https://doi.org/10.1016/s0065-230x\(08\)60970-7](https://doi.org/10.1016/s0065-230x(08)60970-7)
- Siegel, R. L., Miller, K. D., Fuchs, H. E., & Jemal, A. (2022). Cancer statistics, 2022. *CA Cancer J Clin*, 72(1), 7-33. <https://doi.org/10.3322/caac.21708>
- Singal, G., Miller, P. G., Agarwala, V., Li, G., Kaushik, G., Backenroth, D., Gossai, A., Frampton, G. M., Torres, A. Z., Lehnert, E. M., Bourque, D., O'Connell, C., Bowser, B., Caron, T., Baydur, E., Seidl-Rathkopf, K., Ivanov, I., Alpha-Cobb, G., Guria, A., . . . Miller, V. A. (2019). Association of Patient Characteristics and Tumor Genomics With Clinical Outcomes Among Patients With Non-Small Cell Lung Cancer Using a Clinicogenomic Database. *Jama*, 321(14), 1391-1399. <https://doi.org/10.1001/jama.2019.3241>

- Soleymanlou, N., Wu, Y., Wang, J. X., Todros, T., Ietta, F., Jurisicova, A., Post, M., & Caniggia, I. (2005). A novel Mtd splice isoform is responsible for trophoblast cell death in pre-eclampsia. *Cell Death Differ*, *12*(5), 441-452. <https://doi.org/10.1038/sj.cdd.4401593>
- Srivastava, R., Cao, Z., Nedeva, C., Naim, S., Bachmann, D., Rabachini, T., Gangoda, L., Shahi, S., Glab, J., Menassa, J., Osellame, L., Nelson, T., Fernandez-Marrero, Y., Brown, F., Wei, A., Ke, F., O'Reilly, L., Doerflinger, M., Allison, C., . . . Puthalakath, H. (2019). BCL-2 family protein BOK is a positive regulator of uridine metabolism in mammals. *Proc Natl Acad Sci U S A*, *116*(31), 15469-15474. <https://doi.org/10.1073/pnas.1904523116>
- Tago, Y., Yamano, S., Wei, M., Kakehashi, A., Kitano, M., Fujioka, M., Ishii, N., & Wanibuchi, H. (2013). Novel medium-term carcinogenesis model for lung squamous cell carcinoma induced by N-nitroso-tris-chloroethylurea in mice. *Cancer Sci*, *104*(12), 1560-1566. <https://doi.org/10.1111/cas.12289>
- Tantawy, S. I., Timofeeva, N., Sarkar, A., & Gandhi, V. (2023). Targeting MCL-1 protein to treat cancer: opportunities and challenges. *Front Oncol*, *13*, 1226289. <https://doi.org/10.3389/fonc.2023.1226289>
- TCGA Research Network. (2014). Comprehensive molecular profiling of lung adenocarcinoma. *Nature*, *511*(7511), 543-550. <https://doi.org/10.1038/nature13385>
- Thai, A. A., Solomon, B. J., Sequist, L. V., Gainor, J. F., & Heist, R. S. (2021). Lung cancer. *Lancet*, *398*(10299), 535-554. [https://doi.org/10.1016/s0140-6736\(21\)00312-3](https://doi.org/10.1016/s0140-6736(21)00312-3)
- Thunnissen, E. (2012). Pulmonary adenocarcinoma histology. *Transl Lung Cancer Res*, *1*(4), 276-279. <https://doi.org/10.3978/j.issn.2218-6751.2012.10.11>
- Travis, W. D., Brambilla, E., Noguchi, M., Nicholson, A. G., Geisinger, K., Yatabe, Y., Ishikawa, Y., Wistuba, I., Flieder, D. B., Franklin, W., Gazdar, A., Hasleton, P. S., Henderson, D. W., Kerr, K. M., Petersen, I., Roggli, V., Thunnissen, E., & Tsao, M. (2013). Diagnosis of lung cancer in small biopsies and cytology: implications of the 2011 International Association for the Study of Lung Cancer/American Thoracic Society/European Respiratory Society classification. *Arch Pathol Lab Med*, *137*(5), 668-684. <https://doi.org/10.5858/arpa.2012-0263-RA>
- van Meerbeeck, J. P., Fennell, D. A., & De Ruyscher, D. K. (2011). Small-cell lung cancer. *Lancet*, *378*(9804), 1741-1755. [https://doi.org/10.1016/s0140-6736\(11\)60165-7](https://doi.org/10.1016/s0140-6736(11)60165-7)
- Warren, C. F. A., Wong-Brown, M. W., & Bowden, N. A. (2019). BCL-2 family isoforms in apoptosis and cancer. *Cell Death Dis*, *10*(3), 177. <https://doi.org/10.1038/s41419-019-1407-6>
- Winslow, M. M., Dayton, T. L., Verhaak, R. G., Kim-Kiselak, C., Snyder, E. L., Feldser, D. M., Hubbard, D. D., DuPage, M. J., Whittaker, C. A., Hoersch, S., Yoon, S., Crowley, D., Bronson, R. T., Chiang, D. Y., Meyerson, M., & Jacks, T. (2011). Suppression of lung adenocarcinoma progression by Nkx2-1. *Nature*, *473*(7345), 101-104. <https://doi.org/https://doi.org/10.1038/nature09881>
- Wolf, A. M. D., Oeffinger, K. C., Shih, T. Y., Walter, L. C., Church, T. R., Fontham, E. T. H., Elkin, E. B., Etzioni, R. D., Guerra, C. E., Perkins, R. B., Kondo, K. K., Kratzer, T. B., Manassaram-Baptiste, D., Dahut, W. L., & Smith, R. A. (2024). Screening for lung

- cancer: 2023 guideline update from the American Cancer Society. *CA Cancer J Clin*, 74(1), 50-81. <https://doi.org/10.3322/caac.21811>
- Xu, X., Rock, J. R., Lu, Y., Futtner, C., Schwab, B., Guinney, J., Hogan, B. L., & Onaitis, M. W. (2012). Evidence for type II cells as cells of origin of K-Ras-induced distal lung adenocarcinoma. *Proc Natl Acad Sci U S A*, 109(13), 4910-4915. <https://doi.org/10.1073/pnas.1112499109>
- Yakovlev, A. G., Di Giovanni, S., Wang, G., Liu, W., Stoica, B., & Faden, A. I. (2004). BOK and NOXA are essential mediators of p53-dependent apoptosis. *J Biol Chem*, 279(27), 28367-28374. <https://doi.org/10.1074/jbc.M313526200>
- Yip, K. W., & Reed, J. C. (2008). Bcl-2 family proteins and cancer. *Oncogene*, 27(50), 6398-6406. <https://doi.org/10.1038/onc.2008.307>
- Zhang, F., Ren, L., Zhou, S., Duan, P., Xue, J., Chen, H., Feng, Y., Yue, X., Yuan, P., Liu, Q., Yang, P., & Lei, Y. (2019). Role of B-Cell Lymphoma 2 Ovarian Killer (BOK) in Acute Toxicity of Human Lung Epithelial Cells Caused by Cadmium Chloride. *Med Sci Monit*, 25, 5356-5368. <https://doi.org/10.12659/msm.913706>
- Zheng, J. H., Grace, C. R., Guibao, C. D., McNamara, D. E., Llambi, F., Wang, Y. M., Chen, T., & Moldoveanu, T. (2018). Intrinsic Instability of BOK Enables Membrane Permeabilization in Apoptosis. *Cell Rep*, 23(7), 2083-2094.e2086. <https://doi.org/10.1016/j.celrep.2018.04.060>